Study of double parton scattering using W + 2-jet events in proton-proton collisions at $\sqrt{s} = 7\,\text{TeV}$

The CMS collaboration

E-mail: cms-publication-committee-chair@cern.ch

ABSTRACT: Double parton scattering is investigated in proton-proton collisions at $\sqrt{s} = 7\,\text{TeV}$ where the final state includes a W boson, which decays into a muon and a neutrino, and two jets. The data sample corresponds to an integrated luminosity of $5\,\text{fb}^{-1}$, collected with the CMS detector at the LHC. Observables sensitive to double parton scattering are investigated after being corrected for detector effects and selection efficiencies. The fraction of W + 2-jet events due to double parton scattering is measured to be $0.055 \pm 0.002\,(\text{stat.}) \pm 0.014\,(\text{syst.})$. The effective cross section, σ_{eff}, characterizing the effective transverse area of hard partonic interactions in collisions between protons is measured to be $20.7 \pm 0.8\,(\text{stat.}) \pm 6.6\,(\text{syst.})\,\text{mb}$.

Contents

1   Introduction

In high-energy proton-proton (pp) collisions at the Large Hadron Collider (LHC), semi-hard parton-parton scattering, producing particles with transverse momenta p_{T} of a few GeV, dominates the inelastic cross section. In such processes longitudinal momentum fractions, given by $x \sim 2p_{\mathrm{T}}/\sqrt{s}$, of values down to $\mathcal{O}(10^{-3})$ are probed. At these values of x, the parton densities are large causing a sizable probability for two or more parton-parton scatterings within the same pp interaction [1]. Such multi-parton interactions (MPI) at semi-hard scales of a few GeVs have been observed in high-energy hadronic collisions [2]. Conversely, the evidence for hard double parton scattering (DPS) processes in the same pp collision at scales of a few tens of GeV is still relatively weak. In processes where a W and two jets are produced, the x values are larger, $x \sim 10^{-2}$, and the parton densities are lower. However, a sizable contribution to DPS can still be expected if the second scattering, yielding two jets, occurs at a high rate. The study of DPS processes is important because it provides valuable information on the transverse distribution of partons in the proton [3] and
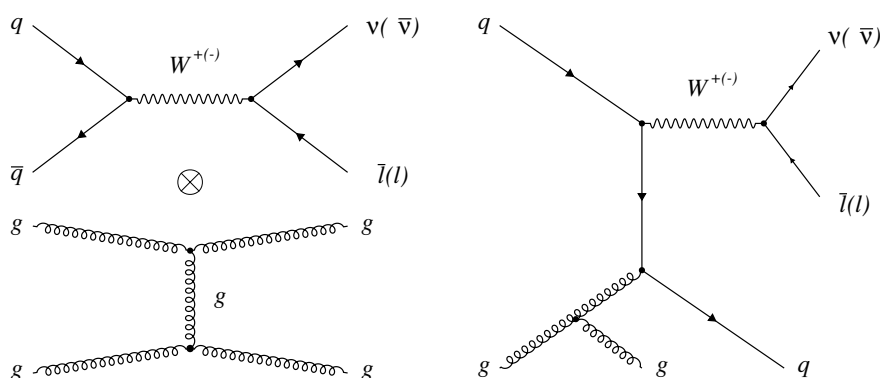
Figure 1. Feynman diagrams for W + 2-jet production from (left) double parton scattering and (right) single parton scattering.

on the multi-parton correlations in the hadronic wave function [4]. DPS also constitutes a background to new physics searches at the LHC [5–7].

Various measurements in pp and p$\bar{\text{p}}$ collisions at $\sqrt{s} = 63\,\text{GeV}$ [8], $630\,\text{GeV}$ [9], and $1.8\,\text{TeV}$ [10] are consistent with DPS contributions to multijet final states, as well as to γ + 3-jet events at $\sqrt{s} = 1.8\,\text{TeV}$ [11] and $1.96\,\text{TeV}$ [12]. Additional searches for DPS have been proposed via double Drell-Yan, four jet, and same-sign WW production, as well as in W production associated with jets [13–20]. This paper presents a study of DPS based on W + 2-jet events in pp collisions at 7 TeV. DPS with a W + 2-jet final state occurs when one hard interaction produces a W boson and another produces a dijet in the same pp collision, as sketched in figure 1(left). The W + 2-jet process is attractive because the muonic decay of the W provides a clean tag and the large dijet production cross section increases the probability of observing DPS. Events containing a W + 2-jet final state originating from single parton scattering (SPS) constitute an irreducible background (figure 1(right)). The ATLAS collaboration has carried out a similar DPS measurement using W + 2-jet events at $\sqrt{s} = 7\,\text{TeV}$ [21].

The outline of this paper is as follows. Section 2 describes DPS in terms of effective cross section and defines the relevant observables. Section 3 presents a brief description of the Compact Muon Solenoid (CMS) detector, the data and the simulated samples, as well as the event selection criteria. Section 4 summarizes the unfolding of the DPS-sensitive observables, the systematic effects, and the comparison of data and simulation. The method to extract the DPS fraction is discussed in section 5. Section 6 presents the extraction of the DPS fraction from the data and corresponding systematic uncertainties. The measurement of the effective cross section is described in section 7.

2 Effective cross section

The effective cross section, σ_{eff}, is a measure of the transverse distribution of partons inside the colliding hadrons and their overlap in a collision. The effective cross section involves the cross section for two processes to occur simultaneously and the cross sections for the

individual processes. If A and B are two independent processes, whose production cross sections are σ_A and σ_B, respectively, σ_{eff} can be written as:

$$\sigma_{\text{eff}} = \frac{m}{2} \frac{\sigma_A \cdot \sigma_B}{\sigma_{A+B}^{DPS}}, \tag{2.1}$$

where "m" is a symmetry factor for indistinguishable ($m = 1$) and distinguishable ($m = 2$) final-states and σ_{A+B}^{DPS} is the cross section of the two processes to occur simultaneously.

According to various phenomenological studies [22–24], the above cross sections should be inclusive. This requirement makes the determination of σ_{eff} independent of the specific mechanisms of the first and second interactions, as well as of the parton distribution functions (PDF). Inclusive σ_{A+B}^{DPS} also includes contributions from higher number of parton scatters.

However, in the present analysis an exclusive selection is performed by considering the events with one W boson and exactly two jets with $p_T > 20\,\text{GeV}/c$ and pseudorapidity, η, within ± 2. The pseudorapidity is defined as $\eta = -\ln[\tan(\theta/2)]$, where θ is the polar angle measured with respect to the anti-clockwise beam direction. This sample should have a significant contribution from events where one interaction produces only a W boson and no jet with $p_T > 20\,\text{GeV}/c$ within $|\eta| < 2.0$ and the other interaction produces exactly two jets with $p_T > 20\,\text{GeV}/c$ and $|\eta| < 2.0$.

Experimentally, the exclusive selection is necessary to identify the jets from the second interaction. In this case, DPS-sensitive observables can be defined based on the back-to-back topology of the two jets. From a sample of simulated events generated with MADGRAPH 5 [25, 26] followed by hadronization and parton showering (PS) using the 4C tune [27] of PYTHIA 8 [28], it is found that σ_{eff} changes by only 2–3% if an inclusive selection is applied.

In order to account for missing contributions of a larger number of parton scatterings, corrections [22–24] were proposed to a previous DPS measurement of CDF [11]. However, in the kinematic region of the present study, due to the requirement of having exactly 2 jets, the contribution of triple and higher number of scatters is expected to be small and is estimated, with the same sample of simulated events as mentioned above, to be less than 1% of the DPS contribution. Therefore, for the present analysis no additional correction is required for the exclusive selection.

Assuming independent interactions from DPS, σ_{eff} can be rewritten in terms of the cross sections at the stable particle level (defined as lifetime, $c\tau > 10$ mm) within the detector acceptance. For the case of the W + 2-jet process, σ_{eff} becomes:

$$\sigma_{\text{eff}} = \frac{\sigma'_{W+0j}}{\sigma'^{DPS}_{W+2j}} \cdot \sigma'_{2j}, \tag{2.2}$$

where the prime indicates that the cross sections are obtained at particle level. The σ'_{W+0j} and σ'_{2j} are the particle-level cross sections for W-boson production associated with zero-jet and for dijet events, respectively. The particle-level cross section for DPS events producing a W + 0-jet from the first interaction and exactly two jets from the second interaction is denoted by σ'^{DPS}_{W+2j}. The cross sections σ'_{W+0j} and σ'^{DPS}_{W+2j} are extracted from the same data

sample; therefore σ_{eff} can be reformulated in terms of the yield of W bosons associated with zero jets and the yield associated with DPS:

$$\sigma_{\text{eff}} = \frac{N'_{\text{W}+0\text{j}}}{N'^{\text{DPS}}_{\text{W}+2\text{j}}} \cdot \sigma'_{2\text{j}}. \tag{2.3}$$

If we define the DPS fraction as

$$f_{\text{DPS}} = \frac{N'^{\text{DPS}}_{\text{W}+2\text{j}}}{N'_{\text{W}+2\text{j}}}, \tag{2.4}$$

σ_{eff} can be written as

$$\sigma_{\text{eff}} = \frac{N'_{\text{W}+0\text{j}}}{f_{\text{DPS}} \cdot N'_{\text{W}+2\text{j}}} \cdot \sigma'_{2\text{j}}, \tag{2.5}$$

or

$$\sigma_{\text{eff}} = \frac{R}{f_{\text{DPS}}} \cdot \sigma'_{2\text{j}}, \tag{2.6}$$

where $R = N'_{\text{W}+0\text{j}}/N'_{\text{W}+2\text{j}}$. Thus, the determination of the effective cross section reduces to a measurement of R, $\sigma'_{2\text{j}}$, and f_{DPS}.

For the extraction of the DPS fraction, f_{DPS}, observables that can discriminate between SPS and DPS are needed. For DPS events, the W and the dijet system are independent of each other, while for SPS events they are highly correlated. It is thus possible to define several observables that discriminate between DPS and SPS events. The present analysis uses the following observables, which were also considered in previous DPS measurements at the LHC and the Tevatron:

- the relative p_{T}-balance between the two jets, $\Delta^{\text{rel}} p_{\text{T}}$, defined as:

$$\Delta^{\text{rel}} p_{\text{T}} = \frac{|\vec{p}_{\text{T}}(\text{j}_1) + \vec{p}_{\text{T}}(\text{j}_2)|}{|\vec{p}_{\text{T}}(\text{j}_1)| + |\vec{p}_{\text{T}}(\text{j}_2)|}. \tag{2.7}$$

Here $\vec{p}_{\text{T}}(\text{j}_1)$ and $\vec{p}_{\text{T}}(\text{j}_2)$ are the transverse momentum vectors of the leading (in p_{T}) and subleading jets. In DPS events, at leading order (LO), the two jets balance each other and $\Delta^{\text{rel}} p_{\text{T}}$ is small, which is not the case for SPS events.

- The azimuthal angle between the W-boson and the dijet system, ΔS, defined as:

$$\Delta\text{S} = \arccos\left(\frac{\vec{p}_{\text{T}}(\mu, \not{E}_{\text{T}}) \cdot \vec{p}_{\text{T}}(\text{j}_1, \text{j}_2)}{|\vec{p}_{\text{T}}(\mu, \not{E}_{\text{T}})| \cdot |\vec{p}_{\text{T}}(\text{j}_1, \text{j}_2)|}\right), \tag{2.8}$$

where $\vec{p}_{\text{T}}(\mu, \not{E}_{\text{T}})$ and $\vec{p}_{\text{T}}(\text{j}_1, \text{j}_2)$ are the combined transverse momentum vectors of $(\mu, \not{E}_{\text{T}})$ and the two jets, respectively, with $\not{E}_{\text{T}}$ as the missing transverse energy in the event, which is a measure of the transverse energy carried away by the neutrino from the W-boson decay. In DPS events, the W and dijet momentum vectors are randomly oriented, whereas in SPS events the W and the dijet momenta vectors tend to be back-to-back at LO.

3 Experimental methods

In the present analysis a sample of W + 2-jet events is selected from a data sample of pp collisions at $\sqrt{s} = 7\,\text{TeV}$ with the CMS detector. The data sample corresponds to an integrated luminosity of $5\,\text{fb}^{-1}$. The distributions are fully corrected for detector effects and efficiencies. These distributions are used for the extraction of the DPS fraction and the determination of the effective cross section. The dijet production cross section required for the determination of the effective cross section is measured with a pp data sample collected in 2010 also at $\sqrt{s} = 7\,\text{TeV}$. This sample corresponds to an integrated luminosity of $35\,\text{pb}^{-1}$.

The central feature of the CMS apparatus is a superconducting solenoid of 6 m internal diameter, providing a magnetic field of 3.8 T. Within the superconducting solenoid volume are a silicon pixel and strip tracker, a lead tungstate crystal electromagnetic calorimeter (ECAL), and a brass/scintillator hadron calorimeter (HCAL). Muons are measured in gas-ionization detectors embedded in the steel flux return yoke outside the solenoid. In addition, CMS has extensive forward calorimetry. The CMS experiment uses a right-handed coordinate system, with the origin at the nominal interaction point, the x axis pointing to the centre of the LHC ring, the y axis pointing up (perpendicular to the plane of the LHC ring), and the z axis along the anticlockwise-beam direction. The polar angle θ is measured from the positive z axis and the azimuthal angle ϕ is measured in the x-y plane. A more detailed description of the CMS apparatus can be found in ref. [29].

3.1 Simulated samples

Samples of W + jets events are generated with MADGRAPH 5 followed by hadronization and parton showering using the Z2 tune [30] of PYTHIA 6 (version 6.4.25) [31]. The MADGRAPH event generator produces parton-level events with a W boson and up to four partons in the final state on the basis of matrix element (ME) calculations. The ME/PS matching scale μ is taken to be 20 GeV, and the factorization and renormalization scales are set to $q^2 = M_W^2 c^2 + (p_T^W)^2$, where M_W and p_T^W are the mass and transverse momentum of the W boson, respectively.

Samples of Z/γ^* + jets and $t\bar{t}$ events are also simulated with MADGRAPH 5. Single-top-quark samples are generated with POWHEG 2 [32]. Samples of WW and WZ events are generated with the PYTHIA 6 Monte Carlo (MC) event generator. Contributions of multijet events from QCD interactions are estimated from data, as discussed later. The inclusive cross sections for simulated processes are normalized to the next-to-leading-order (NLO), next-to-NLO (NNLO), or next-to-next-to-leading-log (NNLL) order calculations. Table 1 gives the values of the cross sections of the simulated processes and their theoretical uncertainties. Theoretical uncertainties have dominant contributions from the PDF uncertainties and the dependence on the renormalization and factorization scales. All simulations are inclusive in terms of final-state partons. Whenever needed, exclusive samples of W + 0-jet and W + 2-jet events are obtained from the inclusive samples by applying selections on the jet multiplicity at the particle and detector levels.

Process	Cross section (pb)
$W \to \mu\nu$	$10500 \pm 5\%$ (NNLO) [33]
$W \to \tau\nu$	$10500 \pm 5\%$ (NNLO) [33]
$t\bar{t}$	$160 \pm 7\%$ (NNLL) [34]
Single top quark	$85 \pm 5\%$ (NLO) [35–37]
Drell-Yan	$3050 \pm 4.3\%$ (NNLO) [33]
Diboson (WW + WZ)	$61 \pm 10\%$ (NLO) [38]
Multijet	Estimated from data by fitting
	$\not{E}_{\mathrm{T}}$ distribution in control region

Table 1. Cross sections of the various processes and their uncertainties.

The simulated samples are processed and reconstructed in the same manner as the collision data. The detector response is simulated in detail by using the GEANT4 package [39]. The samples include additional interactions per beam crossing (the so-called pileup), which match the corresponding distribution in data.

In addition to these fully simulated samples, various simulations at particle level are compared with the fully corrected DPS-sensitive observables.

- MADGRAPH 5 + PYTHIA 8: W + jets events are generated by means of MADGRAPH 5 (as discussed before) followed by hadronization and parton showering using the 4C tune of PYTHIA 8. The MPI [1] are simulated with the PYTHIA 8 event generator. In order to see the effects of MPI, events are also produced without the MPI contribution by PYTHIA 8. For the systematic studies, hadronization and parton showering of MADGRAPH 5 events are performed with PYTHIA 6 tune Z2* [40], with and without MPI.

- POWHEG 2 + PYTHIA 6 (HERWIG 6): W + 2-jet events are also produced up to NLO accuracy with the POWHEG 2 event generator with the "Multi-scale improved NLO" (MiNLO) method [41]. The W + 2-jet samples simulated with the POWHEG 2 + MiNLO describe satisfactorily the inclusive W + jet production data as well [42]. Hadronization and parton showering is carried out with PYTHIA 6, tune Z2*. To assess the effect of angular-ordered showering, HERWIG 6 (version 6.520) [43, 44] is also used for the parton showering.

- PYTHIA 8: W + jets events are generated with the 4C tune of the PYTHIA 8 event generator, which produces hard subprocesses with a W boson and either zero or one additional parton in the final state. It also performs hadronization and parton showering.

The MPI model is similar in PYTHIA 6 and PYTHIA 8, with the free parameters tuned to the underlying event data obtained at the LHC. The key features of the model are:

- the ratio of the 2→2 partonic cross section, integrated above a transverse momentum cutoff scale, to the total inelastic pp cross section, which is a measure of the amount

of MPI. A factor with a free parameter, p_{T0}, is introduced to regularize an otherwise divergent partonic cross section,

$$\frac{\alpha_s^2(p_T^2 + p_{T0}{}^2)}{\alpha_s^2(p_T^2)} \cdot \frac{p_T^4}{(p_T^2 + p_{T0}{}^2)^2} \ , \tag{3.1}$$

with

$$p_{T0}(\sqrt{s}) = p_{T0}(\sqrt{s_0}) \left(\frac{\sqrt{s}}{\sqrt{s_0}} \right)^{\epsilon} \ . \tag{3.2}$$

Here $\sqrt{s_0} = 1.8\,\mathrm{TeV}$ and ϵ is a parameter characterizing the energy dependence of p_{T0}.

- A Poisson distribution for the number of MPI in an event, with a mean that depends on the overlap of the matter distribution of the hadrons in impact parameter space. The impact parameter profile gives a measure of σ_{eff}. The present model uses the convolution of the matter distributions of the two incoming hadrons as an estimate of the impact parameter profile. The overlap function is of the form e^{-bZ}, where b is the impact parameter and Z is a free parameter.

The MPI model used here [31] includes parton showers for the MPI processes as well as MPI processes interleaved with initial state radiation.

Events simulated with LO event generators, i.e. MADGRAPH 5, PYTHIA 6, and PYTHIA 8, use the CTEQ6L [45] PDF set, whereas in the NLO event generation with POWHEG 2 the CTEQ6M [45] PDF set is used.

3.2 Event selection

Events were selected online when at least one muon candidate was found. A muon candidate consists of a track with hits in the muon system and a transverse momentum greater than a threshold. The threshold was increased with increasing instantaneous luminosity in order to keep the rate within the allocated trigger bandwidth for muon triggers. The offline selection requires exactly one muon reconstructed in the muon detector and the silicon tracker. Muon candidates are required to satisfy identification criteria based on the number of hits in the muon detector and the tracker, their transverse impact parameter with respect to the beam axis, and the goodness of the global fit $\chi^2/$(number of degree of freedom) [46] for the tracks in the tracking system and the muon chambers. The background from jets misidentified as muons and from semileptonic decays of heavy quarks is suppressed by applying an isolation condition on the muon candidates. The muon candidate is considered to be isolated if the isolation variable [47], I, is smaller than 0.1.

The selected muon is required to have $p_T > 35\,\mathrm{GeV}/c$ and $|\eta| < 2.1$. The trigger efficiency for the selected muon is larger than 90% and the muon selection efficiency is about 95% [46]. The muon candidate is retained only if associated with the primary vertex identified as the signal vertex. The selected signal vertex is required to be within $\pm 24\,\mathrm{cm}$ of the nominal interaction point along the z direction. At least five tracks are required to be associated with the signal vertex, and the transverse displacement of the signal vertex from the beam axis is required to be less than $2\,\mathrm{cm}$.

Jets and $\not{E}_T$ are reconstructed with the particle-flow (PF) algorithm [48], which combines information from several sub-detectors. The jet reconstruction is based on the anti-k_T clustering algorithm [49–51] with a distance parameter of 0.5. Jets are required to have $p_T > 20\,\mathrm{GeV}/c$ and $|\eta| < 2.0$ to ensure that they are well reconstructed and fall within the tracker acceptance. Jets are required to satisfy identification criteria that eliminate jet candidates originating from noisy channels in the hadron calorimeter [52]. Jet energy scale (JES) corrections are applied to account for the non-linear response of the calorimeters to the particle energy and other instrumental effects. These corrections are based on in-situ measurements using dijet, $\gamma + $ jet, and $Z + $ jet data samples [53]. Pileup and the underlying event can contribute additional energy to the reconstructed jets. The median energy density due to pileup is evaluated in each event and the corresponding energy is subtracted from each jet [54]. Jets are rejected if they overlap with selected muons within a cone of radius 0.5. In order to reject additional jets from pileup interactions, a pileup mitigating variable β is utilized, defined as:

$$\beta = \frac{\Sigma \left(p_T^{\mathrm{signal\ vertex}} \right)}{\Sigma \left(p_T^{\mathrm{all}} \right)}, \tag{3.3}$$

where $\Sigma(p_T^{\mathrm{signal\ vertex}})$ is the sum of the p_T of all charged constituents in a jet associated with the signal vertex and $\Sigma(p_T^{\mathrm{all}})$ is the sum of the p_T of all charged constituents in a jet. Jets are required to have $\beta > 0.4$.

The W transverse mass (M_T) is defined as:

$$M_T = \sqrt{2 \cdot p_T^{\mu} \cdot \not{E}_T \cdot \left(1 - \cos \left(\Delta\phi[\mu, \not{E}_T] \right) \right)}. \tag{3.4}$$

The $\not{E}_T$ is defined as the negative vector sum of the transverse momenta of all reconstructed particle candidates in the event, $\not{E}_T = -\Sigma_i \vec{p}_T(i)$. The reconstructed $\not{E}_T$ is corrected for the non-compensating nature of the calorimeters and detector misalignment using the procedure described in ref. [55]. This procedure uses all corrected jets which have $p_T > 10\,\mathrm{GeV}/c$ and less than 90% of their energy in the ECAL. The $\not{E}_T$ is also corrected for the effect of the azimuthal variation of the tracker acceptance and the calorimeter alignment. The correction factor is calculated as a function of the number of reconstructed vertices and also as a function of ΣE_T, where ΣE_T is the total transverse energy measured in the calorimeter. The angle $\Delta\phi[\mu, \not{E}_T]$ is measured between the muon μ and the $\not{E}_T$ direction in the azimuthal plane.

Events are required to have exactly one muon with $p_T > 35\,\mathrm{GeV}/c$, $|\eta| < 2.1$, and $\not{E}_T > 30\,\mathrm{GeV}$. The transverse mass is required to be greater than $50\,\mathrm{GeV}/c^2$. Selected events are required to have exactly two jets with $p_T > 20\,\mathrm{GeV}/c$ and $|\eta| < 2.0$. The criteria used in the selection are summarized in table 2.

The kinematic distributions of the jets in the selected events are reproduced by the MC simulations as shown in figure 2. Figure 3 shows the comparison of data with MC simulations for $\Delta^{\mathrm{rel}} p_T$ (left) and ΔS (right) at the detector level. Data and MC simulation are in good agreement except for a 10–20% difference at large p_T. This difference is not

W $\rightarrow$ $\mu\nu$ selection	Jet selection
Single-muon trigger	Anti-k_{T} PF jet with $R = 0.5$
Muon ID and isolation	$p_{\mathrm{T}} > 20\,\mathrm{GeV}/c$, $|\eta| < 2.0$
Exactly one muon $p_{\mathrm{T}} > 35\,\mathrm{GeV}/c$, $|\eta| < 2.1$	$\beta > 0.4$
$\not{E}_{\mathrm{T}} > 30\,\mathrm{GeV}/c$	$\Delta R_{\mathrm{j},\mu} > 0.5$
W-boson transverse mass $> 50\,\mathrm{GeV}/c^2$	exactly two jets

Table 2. Summary of the W + 2-jet event selection and reconstruction criteria at the detector level.

Process	Number of events
W $\rightarrow \mu\nu$	$(2.3 \pm 0.12) \times 10^5$
W $\rightarrow \tau\nu$	$(3.7 \pm 0.20) \times 10^3$
Top quark	$(9.4 \pm 0.69) \times 10^3$
Drell-Yan	$(5.3 \pm 0.26) \times 10^3$
Diboson	$(2.6 \pm 0.26) \times 10^3$
Multijet	$(1.1 \pm 0.34) \times 10^3$
Total expected events	$(2.5 \pm 0.14) \times 10^5$
Data	$(2.4 \pm 0.0049) \times 10^5$

Table 3. Expected yields for various processes for $5\,\mathrm{fb}^{-1}$ and observed number of events in the data. The top production background is the sum of the single-top-quark and $t\bar{t}$ processes. The estimated event yields from the simulated samples include uncertainties in the respective cross sections.

a concern for the present analysis because the contribution of events having large p_{T} jet is very small, e.g., only 3% of the W + 2-jet events have a jet p_{T} larger than $100\,\mathrm{GeV}/c$, where the description starts to deviate from the data. There is a small level of background contamination in the selected W + 2-jet samples. The dominant background contribution comes from top-quark production (single top-quark and pair production) and Drell-Yan processes. The contribution of the multijet background is less than 0.5%. This contribution is estimated by defining a control region with the requirement of a non-isolated muon, with $I > 0.1$. A template of the $\not{E}_{\mathrm{T}}$ distribution for the multijet background is constructed by using events in this control region. This template is then used to estimate the contribution of the multijet background by fitting the $\not{E}_{\mathrm{T}}$ distribution in the signal region, with $I < 0.1$. Table 3 summarizes the expected number of events for the processes listed in table 1, for an integrated luminosity of $5\,\mathrm{fb}^{-1}$. The total contribution from the background events is about 10% but the effect on the shape of the DPS-sensitive observables is less than 1%.

4   Unfolding and comparison with simulations

The sample of W + 2-jet events is selected as discussed in the previous section. The contributions of all backgrounds are subtracted from the data distributions before unfolding.
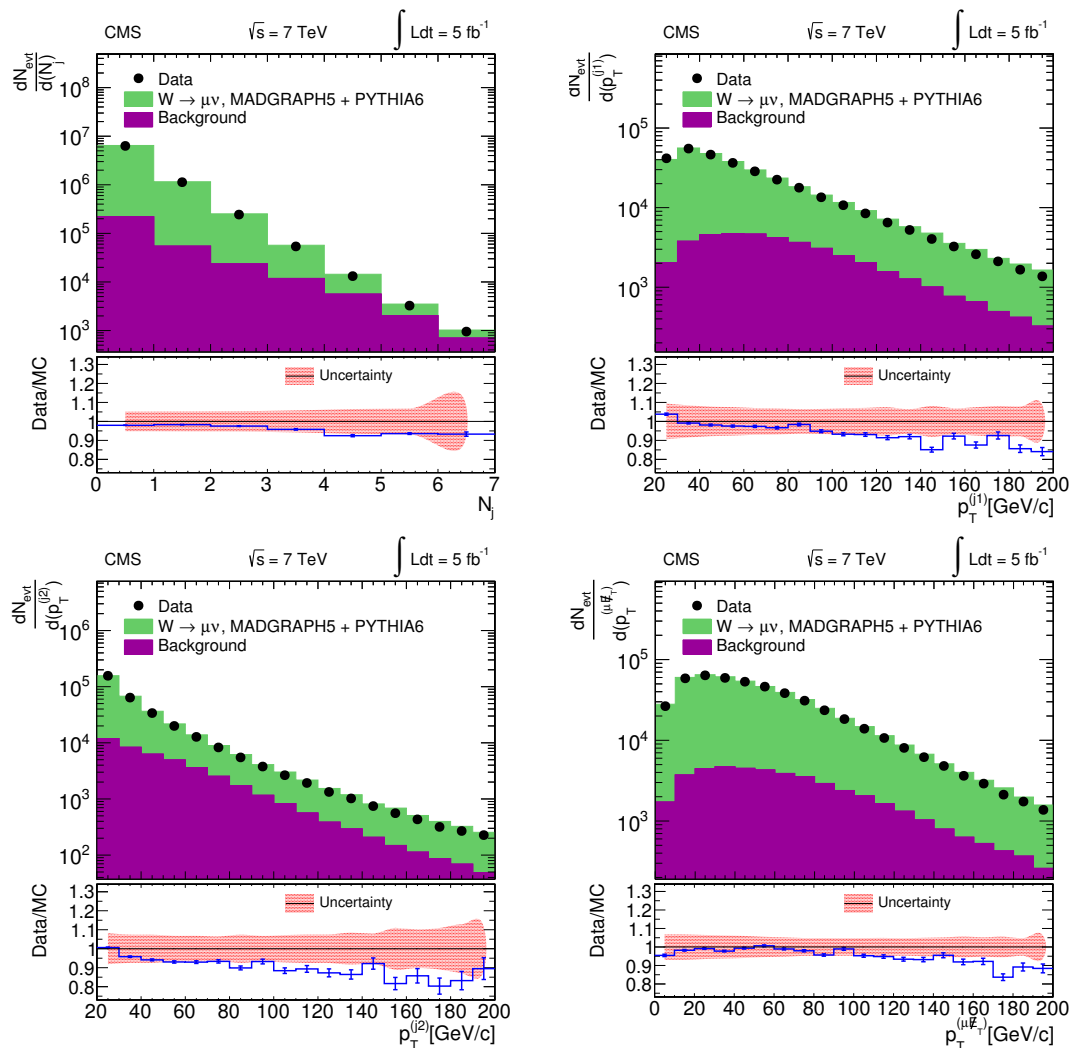
Figure 2. Detector-level comparison of data with MC simulations for the multiplicity (top left) of jets (N_j) with $p_T > 20\,\mathrm{GeV}/c$ and $|\eta| < 2.0$. Data and simulations for the sample with exactly two jets are plotted as a function of the p_T of the leading (top right) and subleading (lower left) jets, as well as of the magnitude of the vector sum of the muon p_T and $\not{E}_T$ (lower right). The background distribution represents the sum of the contributions of Drell-Yan, $W \rightarrow \tau\nu$, diboson, multijet, $t\bar{t}$, and single-top-quark processes. The bottom panels show the ratio of the data and simulated distributions. The band shows the total uncertainty, with the contributions of the jet energy scale uncertainty and the statistical uncertainties of the MC samples added in quadrature. The error bars on the ratio histogram represent the statistical uncertainty of the data and the simulated samples added in quadrature.

The distributions of the DPS-sensitive observables for the selected events are corrected for selection efficiencies and detector effects. The trigger efficiency does not bias the shape of the DPS-sensitive observables; this was checked by comparing simulated samples with and without the trigger requirement. The selected events are mainly SPS events and the sample contains only a few percent of DPS events. However, in the DPS-sensitive region, at low $\Delta^{\mathrm{rel}} p_T$ and ΔS, the DPS contribution is relatively large (a few tens of percent).
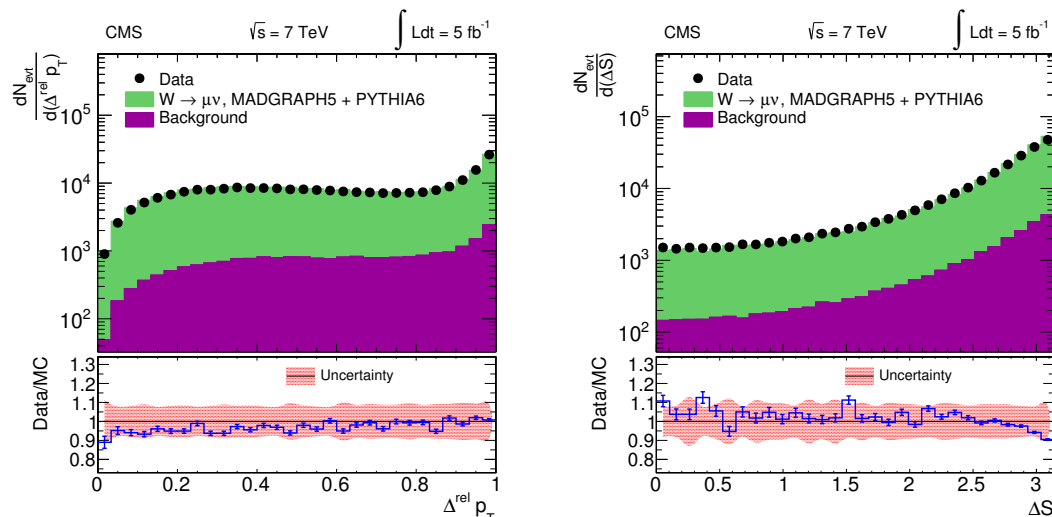
Figure 3. Comparison of data with MC simulations at detector level for the DPS-sensitive observables $\Delta^{\mathrm{rel}} p_T$ (left), and ΔS (right). The background distribution represents the sum of the contributions of Drell-Yan, $W \to \tau\nu$, diboson, multijet, $t\bar{t}$, and single-top-quark processes. The bottom panels show the ratio of the data and simulated distributions. The band shows the total uncertainty, with the contributions of the jet energy scale uncertainty and the statistical uncertainties of the MC samples added in quadrature. The error bars on the ratio histogram represent the statistical uncertainty of the data and the simulated samples added in quadrature.

$1\,\mu: p_T > 35\,\mathrm{GeV}/c$ and $|\eta| < 2.1$
$\displaystyle{\not}E_T > 30\,\mathrm{GeV}$ and $M_T > 50\,\mathrm{GeV}/c^2$
Exactly 2 jets : $p_T > 20\,\mathrm{GeV}/c$ and $|\eta| < 2.0$

Table 4. Phase space definition for the visible cross section at the particle level.

Thus, the shape of the distribution of $\Delta^{\mathrm{rel}} p_T$ and ΔS is more important than the absolute normalization in the extraction of the DPS fraction. Therefore, the unfolding and the systematic studies are carried out for the shapes of the $\Delta^{\mathrm{rel}} p_T$ and ΔS distributions. The measured distributions are unfolded to the level of stable particles (lifetime $c\tau > 10$ mm) within the phase space given in table 4.

Unfolding is performed with an iterative Bayesian method [56] that properly takes into account bin-to-bin migrations. A response matrix is created with simulated events produced with the MADGRAPH 5 + PYTHIA 6 Monte Carlo event generator. The unfolding is cross-checked by using the singular value decomposition (SVD) [57] approach. Iterative Bayesian and SVD approaches give consistent results within uncertainties. Various systematic effects are considered and are listed below:

- *Model dependence:* the sensitivity to the model dependence of the simulations used for the unfolding is estimated by comparing the results unfolded with different MCs. The main effect is due to the simulation of MPI, and is estimated by comparing the detector-level distributions of $\Delta^{\mathrm{rel}} p_T$ and ΔS unfolded by using MADGRAPH 5 + PYTHIA 6, with and without MPI. The effect of removing MPI is about 3–4%,

independent of $\Delta^{\rm rel}\, p_{\rm T}$ and $\Delta{\rm S}$. This is taken as an estimate of the systematic uncertainty due to the model dependence of the simulations.

- *Background subtraction:* the contribution from various backgrounds is estimated with simulated samples that are subtracted from data before applying any corrections. In order to estimate the systematic uncertainties, the cross sections of the background processes are varied within their uncertainties. The shape of the background distribution is affected by the jet energy scale and $\not{E}_{\rm T}$ uncertainties. The total effect of all these uncertainties on the final distribution is less than 0.5%.

- *Jet Energy Scale (JES):* the four momentum of each jet is varied by the JES uncertainty. This variation gives a systematic bias of 1–3%.

- *Jet Energy Resolution (JER):* the JER is different between data and simulation by 3–8% for $|\eta| < 2.0$. A variation of the JER by this amount in the simulation affects the distribution by less than 1%.

- *Resolution of $\not{E}_{\rm T}$:* the $\not{E}_{\rm T}$ resolution differs in data and simulation [55]; this affects the $\Delta{\rm S}$ distribution by at most 3.7%. The effect on the $\Delta^{\rm rel}\, p_{\rm T}$ distribution is less than 1%.

- *Pileup:* in order to take into account the uncertainty in the luminosity measurement [58] and the total inelastic cross section, an uncertainty of 5% is assigned to the mean value of the pileup distribution. This uncertainty affects the $\Delta{\rm S}$ distribution by at most 3.7%, whereas the effect on the $\Delta^{\rm rel}\, p_{\rm T}$ distribution is less than 1%.

Table 5 summarizes the systematic uncertainties for the $\Delta^{\rm rel}\, p_{\rm T}$ and $\Delta{\rm S}$ distributions. The absolute cross section of W + 2-jet events is not important for the extraction of the DPS contribution. However, for completeness the W+ 2-jet production cross section is also corrected to the particle level. The total cross section for the W + 2-jet production (including the DPS contribution), within the region defined in table 4, is measured to be $53.4 \pm 0.1\,({\rm stat.}) \pm 7.6\,({\rm syst.})\,{\rm pb}$. This is consistent with the particle-level prediction by MadGraph 5 + pythia 8, scaled by the ratio of the NNLO and LO cross section for inclusive W production, yielding $55.6 \pm 2.8\,{\rm pb}$. Various systematic effects, arising from the sources discussed above, are also evaluated for the total W + 2-jet cross section. In addition to these, the cross section has a systematic uncertainty of 2.2% due to the luminosity measurement [58]. There is a further uncertainty of 1% in the trigger efficiency and 2% in the muon identification and selection efficiencies [46]. A summary of the various systematic uncertainties for the W + 2-jet cross section is given in the last column of table 5.

A comparison of various simulations for inclusive W production with the corrected distributions is shown in figure 4. The $\Delta^{\rm rel}\, p_{\rm T}$ and $\Delta{\rm S}$ distributions are properly described by MadGraph 5 + pythia 8. MadGraph 5, with hadronization and parton showering carried out with pythia 6, also describes the measurements well. The NLO predictions for W + 2-jet production obtained with powheg 2 + pythia 6 also satisfactorily describe the data. Measurements are also well reproduced by powheg 2, with hadronization and parton showering carried out with herwig 6.

Source	$\Delta^{\rm rel}p_{\rm T}$	$\Delta{\rm S}$	Cross section
Model dependence	≤ 3.2	≤ 3.9	11
Background normalization	≤ 0.2	≤ 0.3	1.0
JES	≤ 1.4	≤ 2.9	7.4
JER	≤ 0.5	≤ 0.7	1.3
$\not{E}_{\rm T}$ scale	≤ 0.5	≤ 3.7	3.3
Pileup	≤ 0.8	≤ 3.7	2.3
Muon ID and trigger	—	—	2.2
Luminosity	—	—	2.2
Total	≤ 3.7	≤ 7.2	14

Table 5. Summary of the systematic uncertainties (in %) for different observables. Uncertainties in integrated luminosity, muon identification (ID), and trigger efficiency only affect the W + 2-jet cross section measurement.

The PYTHIA 8 simulation underestimates the measurements by a factor of 1.5–2.0. This discrepancy is due to the fact that PYTHIA 8 generates only 2→1 and 2→2 processes and most of the additional jets are produced during parton showering, and have a softer $p_{\rm T}$ spectrum than that measured in data. The difference is mainly in the DPS-sensitive region. Therefore, event generators used to define SPS backgrounds must include a proper implementation of additional hard radiation. If it is not included, the effect of missing hard radiation might be interpreted as a DPS contribution. Without MPI, the LO and NLO predictions from MADGRAPH 5 + PYTHIA 8 and POWHEG 2 + PYTHIA 6 are unable to describe the data shown in figure 4. The importance of including MPI, for both LO and NLO simulations in the description of W + 2-jet events, is conclusively shown by the comparisons of data with simulations with and without MPI. In the following sections the contribution of hard MPI is extracted.

5 Strategy for the extraction of the DPS fraction

The fraction of W + 2-jet events produced by DPS is extracted by performing a template fit to the fully corrected distributions of $\Delta^{\rm rel} p_{\rm T}$ and $\Delta{\rm S}$ using a binned likelihood method. Here, the strategy to extract the DPS fraction is discussed, including the definition of the signal and background templates and the corresponding systematic uncertainties.

5.1 DPS signal template

In this analysis, DPS events are required to have one W boson with zero jets from the first interaction and two jets from an independent second interaction, where the jets are required to have $p_{\rm T} > 20\,{\rm GeV}/c$ and $|\eta| < 2.0$. In present analysis, the two interactions are assumed to be independent of each other and a DPS template is produced by randomly mixing W and dijet events. The DPS template is produced by mixing dijet events simulated with
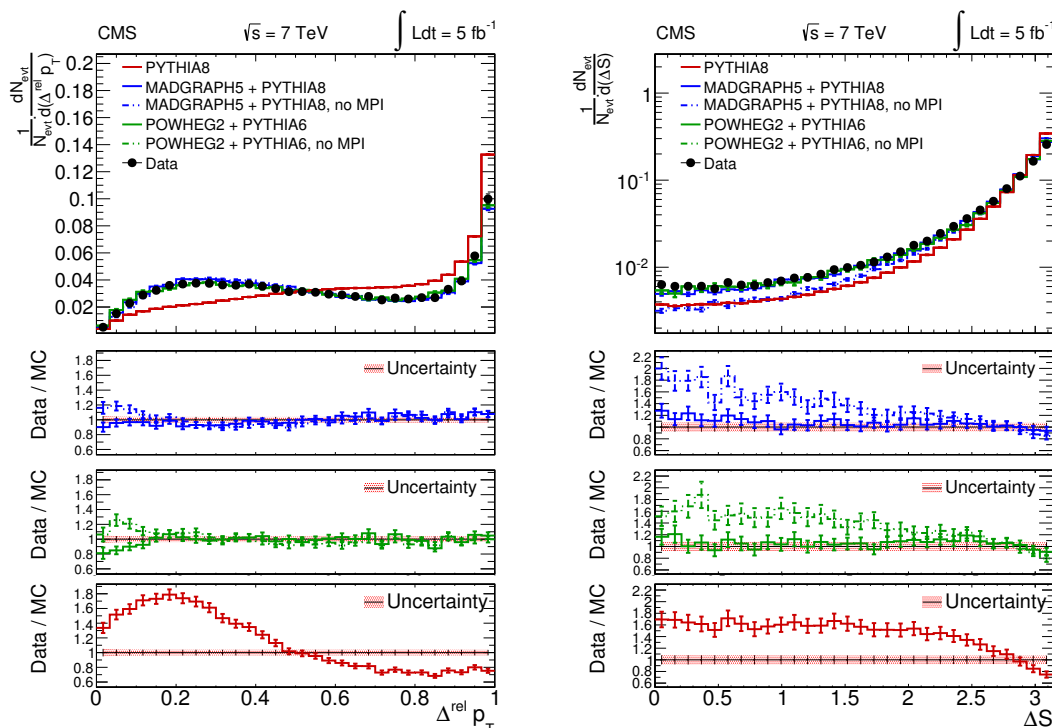
Figure 4. Fully corrected data distributions, normalized to unity, for the DPS-sensitive observables $\Delta^{\rm rel}\,p_{\rm T}$ (left) and ΔS (right). The second panel in both plots shows the ratio of data over MAD-GRAPH 5 + PYTHIA 8 with and without MPI, whereas in the third panel the ratio with POWHEG 2 + PYTHIA 6 is shown. The ratio of the data and PYTHIA 8 is shown in the fourth panel of both plots. The band represents the total uncertainty of the data (cf. table 5).

PYTHIA 8 and W + 0-jet events. These W + 0-jet events are selected as a subsample of the W + jets inclusive sample simulated with MADGRAPH 5 + PYTHIA 8. The DPS templates produced with simulated events are in good agreement with the templates obtained by mixing W + 0-jet and dijet events in the data.

5.2 Background template

In order to construct the background template, inclusive W + jets events are used which are produced with MADGRAPH 5 followed by hadronization and parton showering with PYTHIA 8. The background template cannot be obtained by simply switching off MPI, because only the MPI events that satisfy the DPS signal definition as discussed above need to be excluded. This requires the tagging of the MPI partons and is achieved, in the case of parton showering with PYTHIA 8, by using the status codes 31–39, which are assigned to partons produced from MPI. The background template is constructed by taking inclusive W + jets events that contain exactly two jets with $p_{\rm T} > 20\,{\rm GeV}/c$ and $|\eta| < 2.0$ and by removing those with two MPI tagged partons with $|\eta| < 2.0$. It has been argued [21] that the templates for signal and background must be disjoint and that an additional cutoff on the transverse momentum, $p_{\rm T}^{\rm cut}$, must be applied to the tagged MPI partons. By applying the $p_{\rm T}^{\rm cut}$, events having MPI partons with $p_{\rm T} > p_{\rm T}^{\rm cut}$ are removed from the background
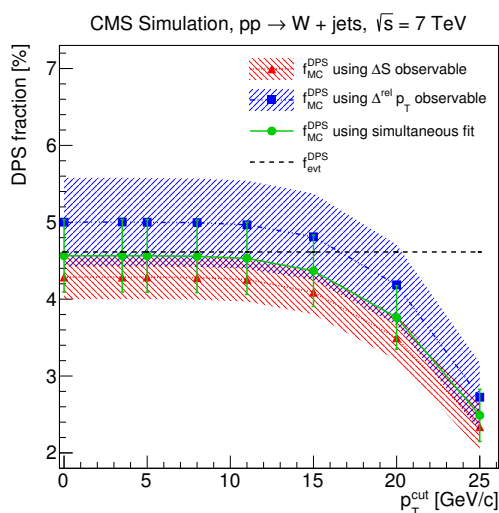
Figure 5. The extracted value of the DPS fraction in W + jets events, simulated with MADGRAPH 5 + PYTHIA 8, using different background templates obtained by varying the transverse momentum cutoff (p_T^{cut}) for the second hard interaction. The DPS fractions obtained by performing both simultaneous and individual fits to the $\Delta^{rel} p_T$ and ΔS observables are shown. The DPS fraction, f_{DPS}^{evt}, for the simulated W + jets events is shown by a dashed black line. The error bars/bands represent the statistical uncertainty added in quadrature to the systematic uncertainty of the DPS template (as discussed in section 6).

template. The effect of applying such a cutoff is studied by comparing at simulation level the fitted and true DPS fraction in the MADGRAPH 5 + PYTHIA 8 sample as a function of p_T^{cut} (figure 5). We observe that, for $p_T^{cut} < 12\,\text{GeV}/c$, the fitted DPS fraction does not depend on p_T^{cut} and therefore we do not apply any cut on p_T of the MPI partons. The true DPS fraction in MADGRAPH 5 + PYTHIA 8 simulation is obtained by counting events containing a W boson and exactly two jets within the acceptance at particle level. The two MPI-tagged partons must also be within the acceptance ($|\eta| < 2.0$) and there must be no parton with $|\eta| < 2.0$ from the first interaction. This fraction, f_{DPS}^{evt}, is determined to be

$$f_{DPS}^{evt} = 0.046 \pm 0.001\,(\text{stat.}). \tag{5.1}$$

Because of the different sensitivities of $\Delta^{rel} p_T$ and ΔS to DPS, the DPS fraction obtained by fitting only the ΔS observable underestimates f_{DPS}^{evt}, whereas the fitted result with $\Delta^{rel} p_T$ overestimates the f_{DPS}^{evt}. However, the fitted DPS fractions are compatible with each other within their systematic uncertainties. In these simulation studies, the main source of systematic bias is the model dependence of the signal templates (a detailed discussion is given in section 6) used for the DPS extraction. If a simultaneous fit of the $\Delta^{rel} p_T$ and ΔS observables is performed, the fitted fraction is consistent with f_{DPS}^{evt}.

The two observables $\Delta^{rel} p_T$ and ΔS are not correlated for signal events; conversely a 40% correlation is present for the background events. The simultaneous fit does not take into account the correlation between the two observables. The possible effect of the correlation is studied with a simulated sample, by extracting the DPS fraction from a fit
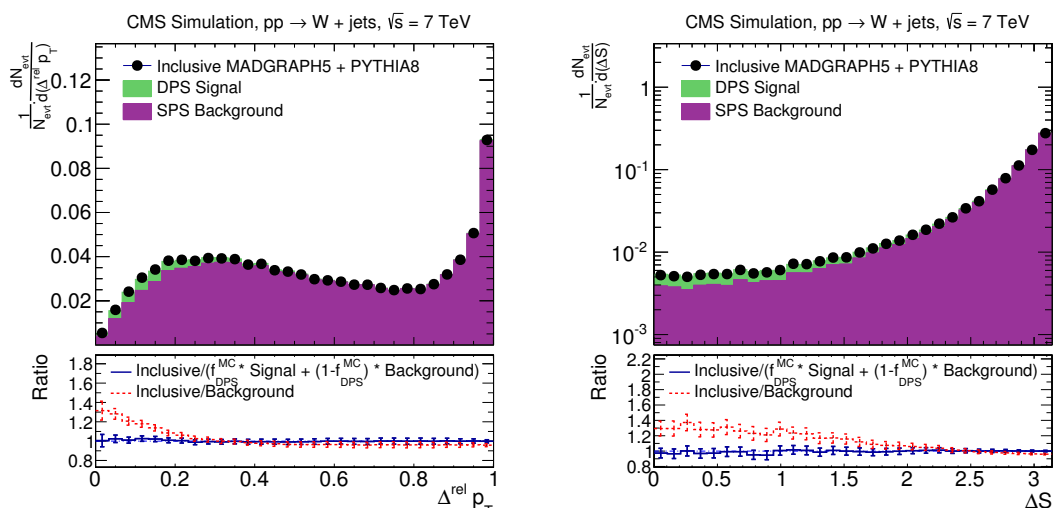
Figure 6. Fit results for the DPS-sensitive observables $\Delta^{\text{rel}} p_{\text{T}}$ (left) and ΔS (right) using signal and background templates. The distributions of the simulated W + 2-jet events are fitted with signal and background templates. The bottom panels show the ratio of the distributions to the fit results. Here, the term "inclusive" means the simulation also includes the DPS contribution.

to the 2-dimensional distribution of $\Delta^{\text{rel}} p_{\text{T}}$ and ΔS. The result differs by 4% from that obtained by simultaneously fitting the two one-dimensional distributions. This effect of the correlation on the DPS fraction is small as compared to the total systematic uncertainty of 26% (as discussed in section 6).

Figure 6 shows the results of fitting the $\Delta^{\text{rel}} p_{\text{T}}$ and ΔS observables for simulated W + 2-jet events with signal and background templates. The extracted DPS fraction in the simulated events is

$$f_{\text{DPS}}^{\text{MC}} = 0.045 \pm 0.002 \text{ (stat.)}, \tag{5.2}$$

which is consistent with the $f_{\text{DPS}}^{\text{evt}}$ value predicted by the default MPI model present in the MADGRAPH 5 + PYTHIA 8 simulation. This closure test also works well when fitting pseudo-data obtained by mixing simulated signal and background events in different proportions.

To summarize, we perform a simultaneous fit of the $\Delta^{\text{rel}} p_{\text{T}}$ and ΔS observables to utilize their different sensitivities and to reduce the uncertainties. The signal template is obtained by randomly mixing independently produced W and dijet events, whereas the background template is produced from the W + 2-jet sample simulated with MADGRAPH 5 + PYTHIA 8, in which events with MPI-tagged partons within the acceptance ($|\eta| < 2.0$) are removed.

6 The DPS fraction in data

The $\Delta^{\text{rel}} p_{\text{T}}$ and ΔS distributions are simultaneously fitted by using the signal and background templates defined in section 5. The fitted value of the DPS fraction (f_{DPS}) is:

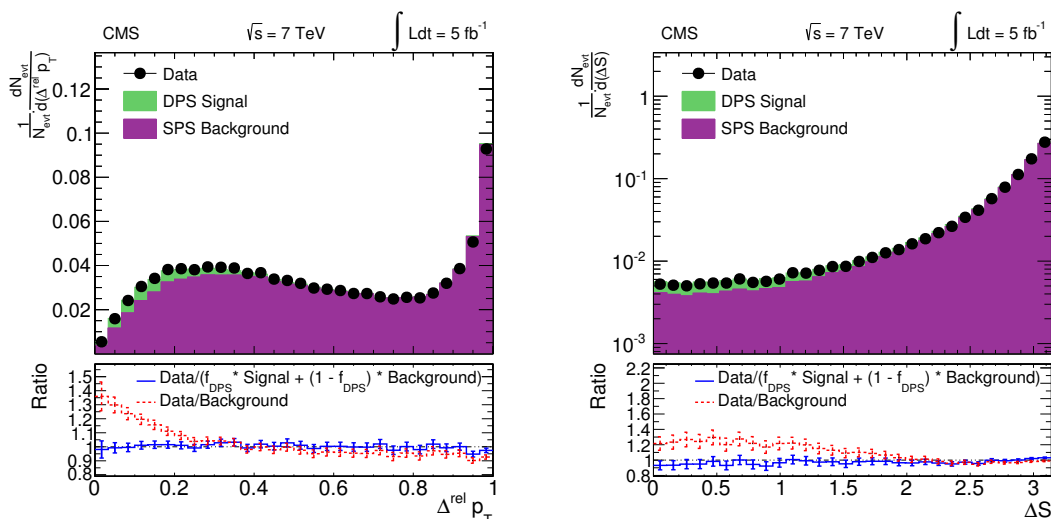$$f_{\text{DPS}} = 0.055 \pm 0.002 \text{ (stat.)} \pm 0.014 \text{ (syst.)}. \tag{6.1}$$

Figure 7. Fit results for the DPS-sensitive observables $\Delta^{\rm rel} p_{\rm T}$ (left) and ΔS (right). Corrected data distributions are fitted with signal and background templates (as discussed in section 5).

The MC predictions using the fit results are shown in figure 7 and compared to data. The following sources of systematic uncertainties are investigated:

- the signal template is generated by randomly mixing W + 0-jet and dijet events from simulated events. The systematic uncertainty in the signal template is calculated by using different simulations for dijet events, i.e. PYTHIA 8, POWHEG 2, and HER-WIG++ [59]. In this signal definition, the first and second interactions are assumed to be completely independent of each other. In order to study possible effects of colour reconnection and energy conservation between the first and the second interactions, an additional cross-check is performed by using the PYTHIA 8 event generator for producing W bosons from the first interaction and the dijet from the second interaction. From figure 4 it has been concluded that PYTHIA 8 fails to describe W + 2-jet measurement due to missing contributions from 2→3 and higher order processes. However, the DPS signal definition only includes W + 0-jet from the first interaction and exactly two jets from the second interaction, which are essentially 2→1 and 2→2 processes, respectively. Therefore, PYTHIA 8 gives a reliable simulation of the DPS signal events. There is a significant contribution from the combinatorial background at particle level, i.e. at least one of the two jets is not from the second interaction. For systematic studies, this combinatorial background is removed by performing jet-parton matching. The variation in the signal template introduces a systematic uncertainty of 9% in the extracted DPS fraction. MPI effects are included in both sets of events used for constructing the signal template; the effect of double counting is studied by switching off MPI in both sets of events, and found to be negligible.

- The background template is generated with MADGRAPH 5 events followed by hadron-ization and parton showering with the PYTHIA 8 event generator. In order to study

the corresponding systematic uncertainty, the background template is obtained from various simulations and parton showering models, i.e. MadGraph 5 + pythia 8, MadGraph 5 + pythia 6 tune Z2*, and powheg 2 + herwig 6. The MPI partons cannot be tagged in pythia 6 and herwig 6. The background template is therefore obtained by switching off MPI. The systematic uncertainty is evaluated by comparing the DPS fractions using different background templates with MPI off. In this procedure, the systematic uncertainty might be overestimated because of the construction of the background templates with simulations in which MPI are turned off. These variations in the background template introduce a systematic uncertainty of 17% in the DPS fraction.

The systematic uncertainty related to the missing higher order diagrams in MadGraph 5 is estimated by varying the QCD renormalization and factorization scales simultaneously up and down by a factor of two. This variation gives a systematic effect of 10% on the extracted value of the DPS fraction.

The ME/PS matching scale is $20\,\mathrm{GeV}$ for the MadGraph 5 + pythia 8 simulation. This p_T-threshold controls the matching of partons produced from the matrix element and that from parton showering. Systematic effects related to the matching scale are estimated by varying the p_T-threshold from $15\,\mathrm{GeV}/c$ to $25\,\mathrm{GeV}/c$. This variation gives a systematic uncertainty of 8% in the DPS fraction.

The total systematic uncertainty on the background template is estimated to be 21%.

- The effect of the uncertainty in PDFs used for the simulated sample is studied by using the PDF reweighting method and the prescription given in ref. [60]. The PDF reweighting only affects the hard scatterings and not the MPI and parton showers. The PDF uncertainties have little effect on the signal template but the variations in the background template result in an uncertainty of 5% in the extracted DPS fraction.

- The systematic uncertainty due to the limited number of simulated events for the background template is obtained by varying the template within its statistical uncertainty. This gives a systematic uncertainty of 5% in the extracted DPS fraction.

- The corrected measured distributions have various systematic uncertainties, as discussed in section 4. The effect of these systematic biases is evaluated by varying the shape of the measured distributions within uncertainties. This variation affects the DPS fraction by 10%.

Table 6 summarizes the various systematic uncertainties in the extracted value of the DPS fraction.

7 Determination of the effective cross section

As discussed in section 2, the effective cross section can be written as

$$\sigma_\mathrm{eff} = \frac{R}{f_\mathrm{DPS}} \cdot \sigma'_\mathrm{2j}. \tag{7.1}$$

Source	Uncertainty (%)
Signal template	9
Background template	21
PDFs	5
Limited MC statistics	5
Uncertainty in corrected data	10
Total	26

Table 6. Systematic uncertainties in the DPS fraction determination.

Source	Uncertainty (%)
Model dependence	9
JES	7
JER	2
Background	2
Pileup	1
Total	12

Table 7. Systematic uncertainties in the measurement of R.

To calculate the effective cross section, in addition to f_{DPS}, the measurements of the dijet cross section and R are also necessary. They are discussed below.

7.1 Measurement of R

The ratio, R, of the yield of events with a W boson in the final state and no jets to the yield of events with a W boson and exactly two jets with $p_{\text{T}} > 20\,\text{GeV}/c$ and $|\eta| < 2.0$ is $25.9 \pm 0.2\,\text{(stat.)}$ at detector level. After subtracting the background contributions from the data, this ratio becomes $27.0 \pm 0.2\,\text{(stat.)}$. The ratio R is unfolded to particle level with a correction factor, $(R^{\text{gen}}/R^{\text{reco}})$, of 1.03 is calculated with MADGRAPH 5 + PYTHIA 6. The corrected value of R is 27.8 with a statistical uncertainty of 0.7%. The measurement of R has a total systematic uncertainty of 12% due to various sources, as listed in table 7. The measured value of R is:

$$R = 27.8 \pm 0.2\,\text{(stat.)} \pm 3.3\,\text{(syst.)}. \qquad (7.2)$$

7.2 Measurement of $\sigma'_{2\text{j}}$

The cross section for dijet production with $p_{\text{T}} > 20\,\text{GeV}/c$ and $|\eta| < 2.0$ ($\sigma'_{2\text{j}}$) is measured with pp collision data at a centre-of-mass energy of 7 TeV collected during 2010. A combination of minimum bias and single-jet triggers is used, as for the inclusive jet cross section measurement [61]. For each trigger, the offline jet p_{T} threshold is chosen such that the trigger is 100% efficient.

Source	Uncertainty (%)
Model dependence	8
JES	13
JER	2
Total	15

Table 8. Uncertainties in the measured value of the dijet cross section.

f_{DPS}	$0.055 \pm 0.002 \,(\text{stat.}) \pm 0.014 \,(\text{syst.})$
R	$27.8 \pm 0.2 \,(\text{stat.}) \pm 3.3 \,(\text{syst.})$
$\sigma'_{2\mathrm{j}}$	$0.0409 \pm 0.0004 \,(\text{stat.}) \pm 0.0061 \,(\text{syst.})\ \text{mb}$
Effective cross section	$20.7 \pm 0.8 \,(\text{stat.}) \pm 6.6 \,(\text{syst.})\ \text{mb}$

Table 9. Measured value of f_{DPS}, R, $\sigma'_{2\mathrm{j}}$, and the effective cross section.

At detector level, the cross section for events with exactly two jets with $p_{\mathrm{T}} > 20\,\text{GeV}/c$ and $|\eta| < 2.0$ is measured to be 0.046 mb. This is corrected to particle level with a correction factor of 0.89 calculated from the PYTHIA 6 simulation. The 8% uncertainty in the correction factor is due to the model dependence, estimated by comparing the corrections obtained from the PYTHIA 6 and HERWIG++ samples. There are further systematic uncertainties of 13% and 2% due to the JES and JER uncertainties, respectively. Table 8 summarizes the various sources of systematic uncertainties. The production cross section $\sigma'_{2\mathrm{j}}$ at particle level is:

$$\sigma'_{2\mathrm{j}} = 0.0409 \pm 0.0004 \,(\text{stat.}) \pm 0.0061 \,(\text{syst.})\ \text{mb}. \tag{7.3}$$

With the values of f_{DPS}, R, and $\sigma'_{2\mathrm{j}}$ in eq. (7.1), the effective cross section is determined to be:

$$\sigma_{\mathrm{eff}} = 20.7 \pm 0.8 \,(\text{stat.}) \pm 6.6 \,(\text{syst.})\ \text{mb}. \tag{7.4}$$

The results of the measurements of R, the DPS fraction, the dijet cross section, and the effective cross section are summarized in table 9. Figure 8 shows a comparison of the effective cross sections obtained using different processes at various centre-of-mass energies. In some theoretical models [22], σ_{eff} is expressed as a simple geometrical integral that is independent of the collision energies. Conversely, PYTHIA predicts an increase of σ_{eff} with centre-of-mass energy because of the parameter $p_{\mathrm{T0}}(\sqrt{s})$, which depends on the collision energy. From the experimental results, a firm conclusion on the energy dependence of σ_{eff} cannot be drawn because of the large systematic uncertainties. The CMS measurement is consistent with previous measurements performed at the Tevatron and by the ATLAS Collaboration at the LHC. The CMS measurement is also consistent with predictions from PYTHIA of 20–30 mb, depending on the tune. The measured effective cross section is also consistent with that obtained by fitting the underlying event data [62] with the HERWIG++ simulation.
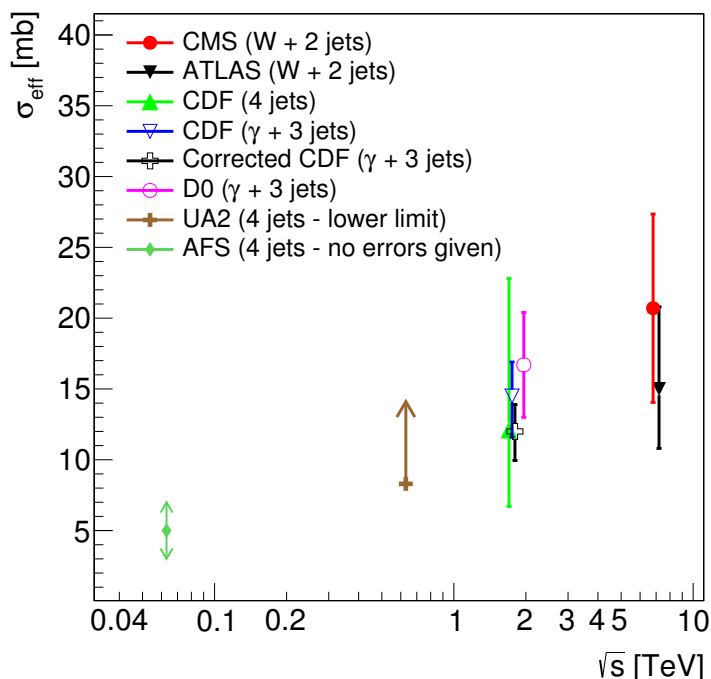
Figure 8. Centre-of-mass energy dependence of σ_{eff} measured by different experiments using different processes [8–12, 21]. These measurements used different approaches for extraction of the DPS fraction and σ_{eff}. The "Corrected CDF" data point indicates the σ_{eff} value corrected for the exclusive event selection [23].

8 Summary

A study of double parton scattering in W + 2-jet events in pp collisions is presented. The data correspond to an integrated luminosity of 5 fb^{-1} collected in pp collisions at a centre-of-mass energy of 7 TeV. Events with a W boson, reconstructed from the muon and $\not{E}_{\text{T}}$ information, are required to have exactly two jets with $p_{\text{T}} > 20\,\text{GeV}/c$ and $|\eta| < 2.0$. The DPS-sensitive observables $\Delta^{\text{rel}}\,p_{\text{T}}$ and ΔS are corrected for detector effects and selection efficiencies. Simulations of W + jets events with MADGRAPH 5 + PYTHIA 8 (or PYTHIA 6) and NLO predictions of POWHEG 2 + PYTHIA 6 (or HERWIG 6) provide a good description of the observables and describe the data only if multiple parton interactions are included.

The fraction of DPS in W + 2-jet events is extracted with a DPS + SPS template fit to the distribution of the $\Delta^{\text{rel}}\,p_{\text{T}}$ and ΔS observables. The obtained value of the DPS fraction is

$$f_{\text{DPS}} = 0.055 \pm 0.002\,(\text{stat.}) \pm 0.014\,(\text{syst.}),\tag{8.1}$$

and the effective cross section, characterizing the effective transverse area of hard partonic interactions in collisions between protons, is calculated to be

$$\sigma_{\text{eff}} = 20.7 \pm 0.8\,(\text{stat.}) \pm 6.6\,(\text{syst.})\,\text{mb}.\tag{8.2}$$

The measured value of the effective cross section is consistent with the Tevatron and ATLAS results.

Acknowledgments

References

[1] T. Sjöstrand and M. van Zijl, *A multiple interaction model for the event structure in hadron collisions*, *Phys. Rev.* **D 36** (1987) 2019 [INSPIRE].

[2] P. Bartalini and L. Fano, *Multiple partonic interactions at the LHC. Proceedings, 1st International Workshop, MPI'08, Perugia, Italy, October 27–31, 2008*, arXiv:1003.4220 [INSPIRE].

[3] M. Diehl, D. Ostermeier and A. Schafer, *Elements of a theory for multiparton interactions in QCD*, *JHEP* **03** (2012) 089 [arXiv:1111.0910] [INSPIRE].

[4] G. Calucci and D. Treleani, *Disentangling correlations in multiple parton interactions*, *Phys. Rev.* **D 83** (2011) 016012 [arXiv:1009.5881] [INSPIRE].

[5] A. Del Fabbro and D. Treleani, *A double parton scattering background to Higgs boson production at the LHC*, *Phys. Rev.* **D 61** (2000) 077502 [hep-ph/9911358] [INSPIRE].

[6] M. Hussein, *A Double parton scattering background to associate WH and ZH production at the LHC*, *Nucl. Phys. Proc. Suppl.* **174** (2007) 55 [hep-ph/0610207] [INSPIRE].

[7] D. Bandurin, G. Golovanov and N. Skachkov, *Double parton interactions as a background to associated HW production at the Tevatron*, *JHEP* **04** (2011) 054 [arXiv:1011.2186] [INSPIRE].

[8] UA2 collaboration, J. Alitti et al., *A study of multi-jet events at the CERN p̄p collider and a search for double parton scattering*, *Phys. Lett.* **B 268** (1991) 145 [INSPIRE].

[9] AXIAL FIELD SPECTROMETER collaboration, T. Akesson et al., *Double parton scattering in pp collisions at $\sqrt{s} = 63\,GeV$*, *Z. Phys.* **C 34** (1987) 163 [INSPIRE].

[10] CDF collaboration, F. Abe et al., *Study of four jet events and evidence for double parton interactions in p̄p collisions at $\sqrt{s} = 1.8\ TeV$*, *Phys. Rev.* **D 47** (1993) 4857 [INSPIRE].

[11] CDF collaboration, F. Abe et al., *Double parton scattering in $\bar{p}p$ collisions at $\sqrt{s} = 1.8\,TeV$*, *Phys. Rev.* **D 56** (1997) 3811 [INSPIRE].

[12] D0 collaboration, V. Abazov et al., *Double parton interactions in photon + 3 jet events in pp^- bar collisions $\sqrt{s} = 1.96$ TeV*, *Phys. Rev.* **D 81** (2010) 052012 [arXiv:0912.5104] [INSPIRE].

[13] C. Goebel, F. Halzen and D.M. Scott, *Double Drell-Yan annihilations in hadron collisions: novel tests of the constituent picture*, *Phys. Rev.* **D 22** (1980) 2789 [INSPIRE].

[14] M. Mekhfi, *Multiparton processes: an application to double Drell-Yan*, *Phys. Rev.* **D 32** (1985) 2371 [INSPIRE].

[15] B. Humpert and R. Odorico, *Multiparton scattering and QCD radiation as sources of four jet events*, *Phys. Lett.* **B 154** (1985) 211 [INSPIRE].

[16] L. Ametller, N. Paver and D. Treleani, *Possible signature of multiple parton interactions in collider four jet events*, *Phys. Lett.* **B 169** (1986) 289 [INSPIRE].

[17] E.L. Berger, C.B. Jackson and G. Shaughnessy, *Characteristics and estimates of double parton scattering at the Large Hadron Collider*, *Phys. Rev.* **D 81** (2010) 014014 [arXiv:0911.5348] [INSPIRE].

[18] R. Godbole, S. Gupta and J. Lindfors, *Double parton scattering contribution to W + jets*, *Z. Phys.* **C 47** (1990) 69 [INSPIRE].

[19] E.L. Berger, C.B. Jackson, S. Quackenbush and G. Shaughnessy, *Calculation of $Wb\bar{b}$ production via double parton scattering at the LHC*, *Phys. Rev.* **D 84** (2011) 074021 [arXiv:1107.3150] [INSPIRE].

[20] J.R. Gaunt, C.-H. Kom, A. Kulesza and W.J. Stirling, *Same-sign W pair production as a probe of double parton scattering at the LHC*, *Eur. Phys. J.* **C 69** (2010) 53 [arXiv:1003.3953] [INSPIRE].

[21] ATLAS collaboration, *Measurement of hard double-parton interactions in $W(\to l\nu) + 2$ jet events at $\sqrt{s} = 7$ TeV with the ATLAS detector*, *New J. Phys.* **15** (2013) 033038 [arXiv:1301.6872] [INSPIRE].

[22] D. Treleani, *Double parton scattering, diffraction and effective cross section*, *Phys. Rev.* **D 76** (2007) 076006 [arXiv:0708.2603] [INSPIRE].

[23] M. Bahr, M. Myska, M.H. Seymour and A. Siodmok, *Extracting $\sigma_{\rm eff}$ from the CDF $\gamma + 3\,jets$ measurement*, *JHEP* **03** (2013) 129 [arXiv:1302.4325] [INSPIRE].

[24] M.H. Seymour and A. Siodmok, *Extracting $\sigma_{\rm eff}$ from the LHCb double-charm measurement*, arXiv:1308.6749 [INSPIRE].

[25] J. Alwall, M. Herquet, F. Maltoni, O. Mattelaer and T. Stelzer, *MadGraph 5: going beyond*, *JHEP* **06** (2011) 128 [arXiv:1106.0522] [INSPIRE].

[26] F. Maltoni and T. Stelzer, *MadEvent: automatic event generation with MadGraph*, *JHEP* **02** (2003) 027 [hep-ph/0208156] [INSPIRE].

[27] R. Corke and T. Sjöstrand, *Interleaved parton showers and tuning prospects*, *JHEP* **03** (2011) 032 [arXiv:1011.1759] [INSPIRE].

[28] T. Sjöstrand, S. Mrenna and P.Z. Skands, *A brief introduction to PYTHIA 8.1*, *Comput. Phys. Commun.* **178** (2008) 852 [arXiv:0710.3820] [INSPIRE].

[29] CMS collaboration, *The CMS experiment at the CERN LHC*, 2008 *JINST* **3** S08004 [INSPIRE].

[30] R. Field, *Early LHC underlying event data — Findings and surprises*, arXiv:1010.3558 [INSPIRE].

[31] T. Sjöstrand, S. Mrenna and P.Z. Skands, *PYTHIA 6.4 physics and manual*, *JHEP* **05** (2006) 026 [hep-ph/0603175] [INSPIRE].

[32] K. Hamilton and P. Nason, *Improving NLO-parton shower matched simulations with higher order matrix elements*, *JHEP* **06** (2010) 039 [arXiv:1004.1764] [INSPIRE].

[33] K. Melnikov and F. Petriello, *Electroweak gauge boson production at hadron colliders through* $O(\alpha_s^2)$, *Phys. Rev.* **D 74** (2006) 114017 [hep-ph/0609070] [INSPIRE].

[34] N. Kidonakis, *Next-to-next-to-leading soft-gluon corrections for the top quark cross section and transverse momentum distribution*, *Phys. Rev.* **D 82** (2010) 114030 [arXiv:1009.4935] [INSPIRE].

[35] N. Kidonakis, *NNLL resummation for s-channel single top quark production*, *Phys. Rev.* **D 81** (2010) 054028 [arXiv:1001.5034] [INSPIRE].

[36] N. Kidonakis, *Next-to-next-to-leading-order collinear and soft gluon corrections for t-channel single top quark production*, *Phys. Rev.* **D 83** (2011) 091503 [arXiv:1103.2792] [INSPIRE].

[37] N. Kidonakis, *Two-loop soft anomalous dimensions for single top quark associated production with a* W^- *or* H^-, *Phys. Rev.* **D 82** (2010) 054018 [arXiv:1005.4451] [INSPIRE].

[38] J.M. Campbell, R.K. Ellis and C. Williams, *Vector boson pair production at the LHC*, *JHEP* **07** (2011) 018 [arXiv:1105.0020] [INSPIRE].

[39] GEANT4 collaboration, S. Agostinelli et al., *GEANT4: a simulation toolkit*, *Nucl. Instrum. Meth.* **A 506** (2003) 250 [INSPIRE].

[40] CMS collaboration, *Study of the underlying event at forward rapidity in pp collisions at* $\sqrt{s} = 0.9$, 2.76 *and 7 TeV*, *JHEP* **04** (2013) 072 [arXiv:1302.2394] [INSPIRE].

[41] K. Hamilton, P. Nason and G. Zanderighi, *MINLO: Multi-scale Improved NLO*, *JHEP* **10** (2012) 155 [arXiv:1206.3572] [INSPIRE].

[42] J.M. Campbell, R.K. Ellis, P. Nason and G. Zanderighi, *W and Z bosons in association with two jets using the POWHEG method*, *JHEP* **08** (2013) 005 [arXiv:1303.5447] [INSPIRE].

[43] G. Marchesini et al., *HERWIG: A Monte Carlo event generator for simulating hadron emission reactions with interfering gluons. Version 5.1 — April 1991*, *Comput. Phys. Commun.* **67** (1992) 465 [INSPIRE].

[44] G. Corcella et al., *HERWIG 6: an event generator for hadron emission reactions with interfering gluons (including supersymmetric processes)*, *JHEP* **01** (2001) 010 [hep-ph/0011363] [INSPIRE].

[45] J. Pumplin et al., *New generation of parton distributions with uncertainties from global QCD analysis*, *JHEP* **07** (2002) 012 [hep-ph/0201195] [INSPIRE].

[46] CMS collaboration, *Measurement of the inclusive W and Z production cross sections in pp collisions at* $\sqrt{s} = 7$ *TeV*, *JHEP* **10** (2011) 132 [arXiv:1107.4789] [INSPIRE].

[47] CMS collaboration, *Measurement of the underlying event in the Drell-Yan process in proton-proton collisions at* $\sqrt{s} = 7$ *TeV*, *Eur. Phys. J.* **C 72** (2012) 2080 [arXiv:1204.1411] [INSPIRE].

[48] CMS collaboration, *Particle-flow event reconstruction in CMS and performance for jets, taus and MET*, CMS-PAS-PFT-09-001 (Particle-Flow Event Reconstruction in CMS and Performance for Jets, Taus and MET).

[49] M. Cacciari, G.P. Salam and G. Soyez, *The anti-k_t jet clustering algorithm*, *JHEP* **04** (2008) 063 [arXiv:0802.1189] [InSPIRE].

[50] M. Cacciari, G.P. Salam and G. Soyez, *FastJet user manual*, *Eur. Phys. J.* **C 72** (2012) 1896 [arXiv:1111.6097] [InSPIRE].

[51] M. Cacciari and G.P. Salam, *Dispelling the N^3 myth for the k_t jet-finder*, *Phys. Lett.* **B 641** (2006) 57 [hep-ph/0512210] [InSPIRE].

[52] CMS collaboration, *Identification and filtering of uncharacteristic noise in the CMS hadron calorimeter*, 2010 *JINST* **5** T03014 [arXiv:0911.4881] [InSPIRE].

[53] CMS collaboration, *Determination of jet energy calibration and transverse momentum resolution in CMS*, 2011 *JINST* **6** P11002 [arXiv:1107.4277] [InSPIRE].

[54] M. Cacciari and G.P. Salam, *Pileup subtraction using jet areas*, *Phys. Lett.* **B 659** (2008) 119 [arXiv:0707.1378] [InSPIRE].

[55] CMS collaboration, *Missing transverse energy performance of the CMS detector*, 2011 *JINST* **6** P09001 [arXiv:1106.5048] [InSPIRE].

[56] G. D'Agostini, *A multidimensional unfolding method based on Bayes' theorem*, *Nucl. Instrum. Meth.* **A 362** (1995) 487 [InSPIRE].

[57] A. Hocker and V. Kartvelishvili, *SVD approach to data unfolding*, *Nucl. Instrum. Meth.* **A 372** (1996) 469 [hep-ph/9509307] [InSPIRE].

[58] CMS collaboration, *Absolute calibration of the luminosity measurement at CMS: winter 2012 update*, CMS-PAS-SMP-12-008 (2012).

[59] M. Bähr et al., *HERWIG++ physics and manual*, *Eur. Phys. J.* **C 58** (2008) 639 [arXiv:0803.0883] [InSPIRE].

[60] S. Alekhin et al., *The PDF4LHC working group interim report*, arXiv:1101.0536 [InSPIRE].

[61] CMS collaboration, *Measurement of the inclusive jet cross section in pp collisions at $\sqrt{s} = 7$ TeV*, *Phys. Rev. Lett.* **107** (2011) 132001 [arXiv:1106.0208] [InSPIRE].

[62] M.H. Seymour and A. Siodmok, *Constraining MPI models using σ_{eff} and recent Tevatron and LHC underlying event data*, *JHEP* **10** (2013) 113 [arXiv:1307.5015] [InSPIRE].

The CMS collaboration

Yerevan Physics Institute, Yerevan, Armenia

S. Chatrchyan, V. Khachatryan, A.M. Sirunyan, A. Tumasyan

Institut für Hochenergiephysik der OeAW, Wien, Austria

W. Adam, T. Bergauer, M. Dragicevic, J. Erö, C. Fabjan[1], M. Friedl, R. Frühwirth[1], V.M. Ghete, C. Hartl, N. Hörmann, J. Hrubec, M. Jeitler[1], W. Kiesenhofer, V. Knünz, M. Krammer[1], I. Krätschmer, D. Liko, I. Mikulec, D. Rabady[2], B. Rahbaran, H. Rohringer, R. Schöfbeck, J. Strauss, A. Taurok, W. Treberer-Treberspurg, W. Waltenberger, C.-E. Wulz[1]

National Centre for Particle and High Energy Physics, Minsk, Belarus

V. Mossolov, N. Shumeiko, J. Suarez Gonzalez

Universiteit Antwerpen, Antwerpen, Belgium

S. Alderweireldt, M. Bansal, S. Bansal, T. Cornelis, E.A. De Wolf, X. Janssen, A. Knutsson, S. Luyckx, L. Mucibello, S. Ochesanu, B. Roland, R. Rougny, H. Van Haevermaet, P. Van Mechelen, N. Van Remortel, A. Van Spilbeeck

Vrije Universiteit Brussel, Brussel, Belgium

F. Blekman, S. Blyweert, J. D'Hondt, N. Heracleous, A. Kalogeropoulos, J. Keaveney, T.J. Kim, S. Lowette, M. Maes, A. Olbrechts, D. Strom, S. Tavernier, W. Van Doninck, P. Van Mulders, G.P. Van Onsem, I. Villella

Université Libre de Bruxelles, Bruxelles, Belgium

C. Caillol, B. Clerbaux, G. De Lentdecker, L. Favart, A.P.R. Gay, A. Léonard, P.E. Marage, A. Mohammadi, L. Perniè, T. Reis, T. Seva, L. Thomas, C. Vander Velde, P. Vanlaer, J. Wang

Ghent University, Ghent, Belgium

V. Adler, K. Beernaert, L. Benucci, A. Cimmino, S. Costantini, S. Dildick, G. Garcia, B. Klein, J. Lellouch, J. Mccartin, A.A. Ocampo Rios, D. Ryckbosch, S. Salva Diblen, M. Sigamani, N. Strobbe, F. Thyssen, M. Tytgat, S. Walsh, E. Yazgan, N. Zaganidis

Université Catholique de Louvain, Louvain-la-Neuve, Belgium

S. Basegmez, C. Beluffi[3], G. Bruno, R. Castello, A. Caudron, L. Ceard, G.G. Da Silveira, C. Delaere, T. du Pree, D. Favart, L. Forthomme, A. Giammanco[4], J. Hollar, P. Jez, M. Komm, V. Lemaitre, J. Liao, O. Militaru, C. Nuttens, D. Pagano, A. Pin, K. Piotrzkowski, A. Popov[5], L. Quertenmont, M. Selvaggi, M. Vidal Marono, J.M. Vizan Garcia

Université de Mons, Mons, Belgium

N. Beliy, T. Caebergs, E. Daubie, G.H. Hammad

Centro Brasileiro de Pesquisas Fisicas, Rio de Janeiro, Brazil

G.A. Alves, M. Correa Martins Junior, T. Martins, M.E. Pol, M.H.G. Souza

Universidade do Estado do Rio de Janeiro, Rio de Janeiro, Brazil

W.L. Aldá Júnior, W. Carvalho, J. Chinellato[6], A. Custódio, E.M. Da Costa, D. De Jesus Damiao, C. De Oliveira Martins, S. Fonseca De Souza, H. Malbouisson, M. Malek, D. Matos Figueiredo, L. Mundim, H. Nogima, W.L. Prado Da Silva, J. Santaolalla, A. Santoro, A. Sznajder, E.J. Tonelli Manganote[6], A. Vilela Pereira

Universidade Estadual Paulista [a], Universidade Federal do ABC [b], São Paulo, Brazil

C.A. Bernardes[b], F.A. Dias[a,7], T.R. Fernandez Perez Tomei[a], E.M. Gregores[b], C. Lagana[a], P.G. Mercadante[b], S.F. Novaes[a], Sandra S. Padula[a]

Institute for Nuclear Research and Nuclear Energy, Sofia, Bulgaria

V. Genchev[2], P. Iaydjiev[2], A. Marinov, S. Piperov, M. Rodozov, G. Sultanov, M. Vutova

University of Sofia, Sofia, Bulgaria

A. Dimitrov, I. Glushkov, R. Hadjiiska, V. Kozhuharov, L. Litov, B. Pavlov, P. Petkov

Institute of High Energy Physics, Beijing, China

J.G. Bian, G.M. Chen, H.S. Chen, M. Chen, R. Du, C.H. Jiang, D. Liang, S. Liang, X. Meng, R. Plestina[8], J. Tao, X. Wang, Z. Wang

State Key Laboratory of Nuclear Physics and Technology, Peking University, Beijing, China

C. Asawatangtrakuldee, Y. Ban, Y. Guo, Q. Li, W. Li, S. Liu, Y. Mao, S.J. Qian, D. Wang, L. Zhang, W. Zou

Universidad de Los Andes, Bogota, Colombia

C. Avila, C.A. Carrillo Montoya, L.F. Chaparro Sierra, C. Florez, J.P. Gomez, B. Gomez Moreno, J.C. Sanabria

Technical University of Split, Split, Croatia

N. Godinovic, D. Lelas, D. Polic, I. Puljak

University of Split, Split, Croatia

Z. Antunovic, M. Kovac

Institute Rudjer Boskovic, Zagreb, Croatia

V. Brigljevic, K. Kadija, J. Luetic, D. Mekterovic, S. Morovic, L. Tikvica

University of Cyprus, Nicosia, Cyprus

A. Attikis, G. Mavromanolakis, J. Mousa, C. Nicolaou, F. Ptochos, P.A. Razis

Charles University, Prague, Czech Republic

M. Finger, M. Finger Jr.

Academy of Scientific Research and Technology of the Arab Republic of Egypt, Egyptian Network of High Energy Physics, Cairo, Egypt

A.A. Abdelalim[9], Y. Assran[10], S. Elgammal[9], A. Ellithi Kamel[11], M.A. Mahmoud[12], A. Radi[13,14]

National Institute of Chemical Physics and Biophysics, Tallinn, Estonia

M. Kadastik, M. Müntel, M. Murumaa, M. Raidal, L. Rebane, A. Tiko

Department of Physics, University of Helsinki, Helsinki, Finland

P. Eerola, G. Fedi, M. Voutilainen

Helsinki Institute of Physics, Helsinki, Finland

J. Härkönen, V. Karimäki, R. Kinnunen, M.J. Kortelainen, T. Lampén, K. Lassila-Perini, S. Lehti, T. Lindén, P. Luukka, T. Mäenpää, T. Peltola, E. Tuominen, J. Tuominiemi, E. Tuovinen, L. Wendland

Lappeenranta University of Technology, Lappeenranta, Finland

T. Tuuva

DSM/IRFU, CEA/Saclay, Gif-sur-Yvette, France

M. Besancon, F. Couderc, M. Dejardin, D. Denegri, B. Fabbro, J.L. Faure, F. Ferri, S. Ganjour, A. Givernaud, P. Gras, G. Hamel de Monchenault, P. Jarry, E. Locci, J. Malcles, A. Nayak, J. Rander, A. Rosowsky, M. Titov

Laboratoire Leprince-Ringuet, Ecole Polytechnique, IN2P3-CNRS, Palaiseau, France

S. Baffioni, F. Beaudette, P. Busson, C. Charlot, N. Daci, T. Dahms, M. Dalchenko, L. Dobrzynski, A. Florent, R. Granier de Cassagnac, P. Miné, C. Mironov, I.N. Naranjo, M. Nguyen, C. Ochando, P. Paganini, D. Sabes, R. Salerno, Y. Sirois, C. Veelken, Y. Yilmaz, A. Zabi

Institut Pluridisciplinaire Hubert Curien, Université de Strasbourg, Université de Haute Alsace Mulhouse, CNRS/IN2P3, Strasbourg, France

J.-L. Agram[15], J. Andrea, D. Bloch, J.-M. Brom, E.C. Chabert, C. Collard, E. Conte[15], F. Drouhin[15], J.-C. Fontaine[15], D. Gelé, U. Goerlach, C. Goetzmann, P. Juillot, A.-C. Le Bihan, P. Van Hove

Centre de Calcul de l'Institut National de Physique Nucleaire et de Physique des Particules, CNRS/IN2P3, Villeurbanne, France

S. Gadrat

Université de Lyon, Université Claude Bernard Lyon 1, CNRS-IN2P3, Institut de Physique Nucléaire de Lyon, Villeurbanne, France

S. Beauceron, N. Beaupere, G. Boudoul, S. Brochet, J. Chasserat, R. Chierici, D. Contardo, P. Depasse, H. El Mamouni, J. Fan, J. Fay, S. Gascon, M. Gouzevitch, B. Ille, T. Kurca, M. Lethuillier, L. Mirabito, S. Perries, J.D. Ruiz Alvarez, L. Sgandurra, V. Sordini, M. Vander Donckt, P. Verdier, S. Viret, H. Xiao

Institute of High Energy Physics and Informatization, Tbilisi State University, Tbilisi, Georgia

Z. Tsamalaidze[16]

RWTH Aachen University, I. Physikalisches Institut, Aachen, Germany

C. Autermann, S. Beranek, M. Bontenackels, B. Calpas, M. Edelhoff, L. Feld, O. Hindrichs, K. Klein, A. Ostapchuk, A. Perieanu, F. Raupach, J. Sammet, S. Schael, D. Sprenger, H. Weber, B. Wittmer, V. Zhukov[5]

RWTH Aachen University, III. Physikalisches Institut A, Aachen, Germany

M. Ata, J. Caudron, E. Dietz-Laursonn, D. Duchardt, M. Erdmann, R. Fischer, A. Güth, T. Hebbeker, C. Heidemann, K. Hoepfner, D. Klingebiel, S. Knutzen, P. Kreuzer, M. Merschmeyer, A. Meyer, M. Olschewski, K. Padeken, P. Papacz, H. Reithler, S.A. Schmitz, L. Sonnenschein, D. Teyssier, S. Thüer, M. Weber

RWTH Aachen University, III. Physikalisches Institut B, Aachen, Germany

V. Cherepanov, Y. Erdogan, G. Flügge, H. Geenen, M. Geisler, W. Haj Ahmad, F. Hoehle, B. Kargoll, T. Kress, Y. Kuessel, J. Lingemann[2], A. Nowack, I.M. Nugent, L. Perchalla, O. Pooth, A. Stahl

Deutsches Elektronen-Synchrotron, Hamburg, Germany

I. Asin, N. Bartosik, J. Behr, W. Behrenhoff, U. Behrens, A.J. Bell, M. Bergholz[17], A. Bethani, K. Borras, A. Burgmeier, A. Cakir, L. Calligaris, A. Campbell, S. Choudhury, F. Costanza, C. Diez Pardos, S. Dooling, T. Dorland, G. Eckerlin, D. Eckstein, T. Eichhorn, G. Flucke, A. Geiser, A. Grebenyuk, P. Gunnellini, S. Habib, J. Hauk, G. Hellwig, M. Hempel, D. Horton, H. Jung, M. Kasemann, P. Katsas, J. Kieseler, C. Kleinwort, M. Krämer, D. Krücker, W. Lange, J. Leonard, K. Lipka, W. Lohmann[17], B. Lutz, R. Mankel, I. Marfin, I.-A. Melzer-Pellmann, A.B. Meyer, J. Mnich, A. Mussgiller, S. Naumann-Emme, O. Novgorodova, F. Nowak, H. Perrey, A. Petrukhin, D. Pitzl, R. Placakyte, A. Raspereza, P.M. Ribeiro Cipriano, C. Riedl, E. Ron, M.Ö. Sahin, J. Salfeld-Nebgen, P. Saxena, R. Schmidt[17], T. Schoerner-Sadenius, M. Schröder, M. Stein, A.D.R. Vargas Trevino, R. Walsh, C. Wissing

University of Hamburg, Hamburg, Germany

M. Aldaya Martin, V. Blobel, H. Enderle, J. Erfle, E. Garutti, K. Goebel, M. Görner, M. Gosselink, J. Haller, R.S. Höing, H. Kirschenmann, R. Klanner, R. Kogler, J. Lange, I. Marchesini, J. Ott, T. Peiffer, N. Pietsch, D. Rathjens, C. Sander, H. Schettler, P. Schleper, E. Schlieckau, A. Schmidt, M. Seidel, J. Sibille[18], V. Sola, H. Stadie, G. Steinbrück, D. Troendle, E. Usai, L. Vanelderen

Institut für Experimentelle Kernphysik, Karlsruhe, Germany

C. Barth, C. Baus, J. Berger, C. Böser, E. Butz, T. Chwalek, W. De Boer, A. Descroix, A. Dierlamm, M. Feindt, M. Guthoff[2], F. Hartmann[2], T. Hauth[2], H. Held, K.H. Hoffmann, U. Husemann, I. Katkov[5], A. Kornmayer[2], E. Kuznetsova, P. Lobelle Pardo, D. Martschei, M.U. Mozer, Th. Müller, M. Niegel, A. Nürnberg, O. Oberst, G. Quast, K. Rabbertz, F. Ratnikov, S. Röcker, F.-P. Schilling, G. Schott, H.J. Simonis, F.M. Stober, R. Ulrich, J. Wagner-Kuhr, S. Wayand, T. Weiler, R. Wolf, M. Zeise

Institute of Nuclear and Particle Physics (INPP), NCSR Demokritos, Aghia Paraskevi, Greece

G. Anagnostou, G. Daskalakis, T. Geralis, S. Kesisoglou, A. Kyriakis, D. Loukas, A. Markou, C. Markou, E. Ntomari, A. Psallidas, I. Topsis-giotis

University of Athens, Athens, Greece

L. Gouskos, A. Panagiotou, N. Saoulidou, E. Stiliaris

University of Ioánnina, Ioánnina, Greece

X. Aslanoglou, I. Evangelou, G. Flouris, C. Foudas, P. Kokkas, N. Manthos, I. Papadopoulos, E. Paradas

Wigner Research Centre for Physics, Budapest, Hungary

G. Bencze, C. Hajdu, P. Hidas, D. Horvath[19], F. Sikler, V. Veszpremi, G. Vesztergombi[20], A.J. Zsigmond

Institute of Nuclear Research ATOMKI, Debrecen, Hungary

N. Beni, S. Czellar, J. Molnar, J. Palinkas, Z. Szillasi

University of Debrecen, Debrecen, Hungary

J. Karancsi, P. Raics, Z.L. Trocsanyi, B. Ujvari

National Institute of Science Education and Research, Bhubaneswar, India

S.K. Swain

Panjab University, Chandigarh, India

S.B. Beri, V. Bhatnagar, N. Dhingra, R. Gupta, M. Kaur, R. Kumar, M. Mittal, N. Nishu, A. Sharma, J.B. Singh

University of Delhi, Delhi, India

Ashok Kumar, Arun Kumar, S. Ahuja, A. Bhardwaj, B.C. Choudhary, A. Kumar, S. Malhotra, M. Naimuddin, K. Ranjan, V. Sharma, R.K. Shivpuri

Saha Institute of Nuclear Physics, Kolkata, India

S. Banerjee, S. Bhattacharya, K. Chatterjee, S. Dutta, B. Gomber, Sa. Jain, Sh. Jain, R. Khurana, A. Modak, S. Mukherjee, D. Roy, S. Sarkar, M. Sharan, A.P. Singh

Bhabha Atomic Research Centre, Mumbai, India

A. Abdulsalam, D. Dutta, S. Kailas, V. Kumar, A.K. Mohanty[2], L.M. Pant, P. Shukla, A. Topkar

Tata Institute of Fundamental Research - EHEP, Mumbai, India

T. Aziz, R.M. Chatterjee, S. Ganguly, S. Ghosh, M. Guchait[21], A. Gurtu[22], G. Kole, S. Kumar, M. Maity[23], G. Majumder, K. Mazumdar, G.B. Mohanty, B. Parida, K. Sudhakar, N. Wickramage[24]

Tata Institute of Fundamental Research - HECR, Mumbai, India

S. Banerjee, S. Dugad

Institute for Research in Fundamental Sciences (IPM), Tehran, Iran

H. Arfaei, H. Bakhshiansohi, H. Behnamian, S.M. Etesami[25], A. Fahim[26], A. Jafari, M. Khakzad, M. Mohammadi Najafabadi, M. Naseri, S. Paktinat Mehdiabadi, B. Safarzadeh[27], M. Zeinali

University College Dublin, Dublin, Ireland

M. Grunewald

INFN Sezione di Bari [a], Università di Bari [b], Politecnico di Bari [c], Bari, Italy

M. Abbrescia[a,b], L. Barbone[a,b], C. Calabria[a,b], S.S. Chhibra[a,b], A. Colaleo[a], D. Creanza[a,c], N. De Filippis[a,c], M. De Palma[a,b], L. Fiore[a], G. Iaselli[a,c], G. Maggi[a,c], M. Maggi[a], B. Marangelli[a,b], S. My[a,c], S. Nuzzo[a,b], N. Pacifico[a], A. Pompili[a,b], G. Pugliese[a,c], R. Radogna[a,b], G. Selvaggi[a,b], L. Silvestris[a], G. Singh[a,b], R. Venditti[a,b], P. Verwilligen[a], G. Zito[a]

INFN Sezione di Bologna [a], Università di Bologna [b], Bologna, Italy

G. Abbiendi[a], A.C. Benvenuti[a], D. Bonacorsi[a,b], S. Braibant-Giacomelli[a,b], L. Brigliadori[a,b], R. Campanini[a,b], P. Capiluppi[a,b], A. Castro[a,b], F.R. Cavallo[a], G. Codispoti[a,b], M. Cuffiani[a,b], G.M. Dallavalle[a], F. Fabbri[a], A. Fanfani[a,b], D. Fasanella[a,b], P. Giacomelli[a], C. Grandi[a], L. Guiducci[a,b], S. Marcellini[a], G. Masetti[a], M. Meneghelli[a,b], A. Montanari[a], F.L. Navarria[a,b], F. Odorici[a], A. Perrotta[a], F. Primavera[a,b], A.M. Rossi[a,b], T. Rovelli[a,b], G.P. Siroli[a,b], N. Tosi[a,b], R. Travaglini[a,b]

INFN Sezione di Catania [a], Università di Catania [b], CSFNSM [c], Catania, Italy

S. Albergo[a,b], G. Cappello[a], M. Chiorboli[a,b], S. Costa[a,b], F. Giordano[a,2], R. Potenza[a,b], A. Tricomi[a,b], C. Tuve[a,b]

INFN Sezione di Firenze [a], Università di Firenze [b], Firenze, Italy

G. Barbagli[a], V. Ciulli[a,b], C. Civinini[a], R. D'Alessandro[a,b], E. Focardi[a,b], E. Gallo[a], S. Gonzi[a,b], V. Gori[a,b], P. Lenzi[a,b], M. Meschini[a], S. Paoletti[a], G. Sguazzoni[a], A. Tropiano[a,b]

INFN Laboratori Nazionali di Frascati, Frascati, Italy

L. Benussi, S. Bianco, F. Fabbri, D. Piccolo

INFN Sezione di Genova [a], Università di Genova [b], Genova, Italy

P. Fabbricatore[a], R. Ferretti[a,b], F. Ferro[a], M. Lo Vetere[a,b], R. Musenich[a], E. Robutti[a], S. Tosi[a,b]

INFN Sezione di Milano-Bicocca [a], Università di Milano-Bicocca [b], Milano, Italy

A. Benaglia[a], M.E. Dinardo[a,b], S. Fiorendi[a,b,2], S. Gennai[a], A. Ghezzi[a,b], P. Govoni[a,b], M.T. Lucchini[a,b,2], S. Malvezzi[a], R.A. Manzoni[a,b,2], A. Martelli[a,b,2], D. Menasce[a], L. Moroni[a], M. Paganoni[a,b], D. Pedrini[a], S. Ragazzi[a,b], N. Redaelli[a], T. Tabarelli de Fatis[a,b]

INFN Sezione di Napoli ^{a}, Università di Napoli 'Federico II' ^{b}, Università della Basilicata (Potenza) ^{c}, Università G. Marconi (Roma) ^{d}, Napoli, Italy

S. Buontempo^a, N. Cavallo^{a,c}, F. Fabozzi^{a,c}, A.O.M. Iorio^{a,b}, L. Lista^a, S. Meola^{a,d,2}, M. Merola^a, P. Paolucci^{a,2}

INFN Sezione di Padova ^{a}, Università di Padova ^{b}, Università di Trento (Trento) ^{c}, Padova, Italy

P. Azzi^a, N. Bacchetta^a, D. Bisello^{a,b}, A. Branca^{a,b}, R. Carlin^{a,b}, T. Dorigo^a, U. Dosselli^a, M. Galanti^{a,b,2}, F. Gasparini^{a,b}, U. Gasparini^{a,b}, P. Giubilato^{a,b}, F. Gonella^a, A. Gozzelino^a, K. Kanishchev^{a,c}, S. Lacaprara^a, I. Lazzizzera^{a,c}, M. Margoni^{a,b}, F. Montecassiano^a, J. Pazzini^{a,b}, N. Pozzobon^{a,b}, P. Ronchese^{a,b}, M. Sgaravatto^a, F. Simonetto^{a,b}, E. Torassa^a, M. Tosi^{a,b}, S. Vanini^{a,b}, P. Zotto^{a,b}, A. Zucchetta^{a,b}, G. Zumerle^{a,b}

INFN Sezione di Pavia ^{a}, Università di Pavia ^{b}, Pavia, Italy

M. Gabusi^{a,b}, S.P. Ratti^{a,b}, C. Riccardi^{a,b}, P. Vitulo^{a,b}

INFN Sezione di Perugia ^{a}, Università di Perugia ^{b}, Perugia, Italy

M. Biasini^{a,b}, G.M. Bilei^a, L. Fanò^{a,b}, P. Lariccia^{a,b}, G. Mantovani^{a,b}, M. Menichelli^a, F. Romeo^{a,b}, A. Saha^a, A. Santocchia^{a,b}, A. Spiezia^{a,b}

INFN Sezione di Pisa ^{a}, Università di Pisa ^{b}, Scuola Normale Superiore di Pisa ^{c}, Pisa, Italy

K. Androsov^{a,28}, P. Azzurri^a, G. Bagliesi^a, J. Bernardini^a, T. Boccali^a, G. Broccolo^{a,c}, R. Castaldi^a, M.A. Ciocci^{a,28}, R. Dell'Orso^a, F. Fiori^{a,c}, L. Foà^{a,c}, A. Giassi^a, M.T. Grippo^{a,28}, A. Kraan^a, F. Ligabue^{a,c}, T. Lomtadze^a, L. Martini^{a,b}, A. Messineo^{a,b}, C.S. Moon^{a,29}, F. Palla^a, A. Rizzi^{a,b}, A. Savoy-Navarro^{a,30}, A.T. Serban^a, P. Spagnolo^a, P. Squillacioti^{a,28}, R. Tenchini^a, G. Tonelli^{a,b}, A. Venturi^a, P.G. Verdini^a, C. Vernieri^{a,c}

INFN Sezione di Roma ^{a}, Università di Roma ^{b}, Roma, Italy

L. Barone^{a,b}, F. Cavallari^a, D. Del Re^{a,b}, M. Diemoz^a, M. Grassi^{a,b}, C. Jorda^a, E. Longo^{a,b}, F. Margaroli^{a,b}, P. Meridiani^a, F. Micheli^{a,b}, S. Nourbakhsh^{a,b}, G. Organtini^{a,b}, R. Paramatti^a, S. Rahatlou^{a,b}, C. Rovelli^a, L. Soffi^{a,b}, P. Traczyk^{a,b}

INFN Sezione di Torino ^{a}, Università di Torino ^{b}, Università del Piemonte Orientale (Novara) ^{c}, Torino, Italy

N. Amapane^{a,b}, R. Arcidiacono^{a,c}, S. Argiro^{a,b}, M. Arneodo^{a,c}, R. Bellan^{a,b}, C. Biino^a, N. Cartiglia^a, S. Casasso^{a,b}, M. Costa^{a,b}, A. Degano^{a,b}, N. Demaria^a, C. Mariotti^a, S. Maselli^a, E. Migliore^{a,b}, V. Monaco^{a,b}, M. Musich^a, M.M. Obertino^{a,c}, G. Ortona^{a,b}, L. Pacher^{a,b}, N. Pastrone^a, M. Pelliccioni^{a,2}, A. Potenza^{a,b}, A. Romero^{a,b}, M. Ruspa^{a,c}, R. Sacchi^{a,b}, A. Solano^{a,b}, A. Staiano^a, U. Tamponi^a

INFN Sezione di Trieste ^{a}, Università di Trieste ^{b}, Trieste, Italy

S. Belforte^a, V. Candelise^{a,b}, M. Casarsa^a, F. Cossutti^a, G. Della Ricca^{a,b}, B. Gobbo^a, C. La Licata^{a,b}, M. Marone^{a,b}, D. Montanino^{a,b}, A. Penzo^a, A. Schizzi^{a,b}, T. Umer^{a,b}, A. Zanetti^a

Kangwon National University, Chunchon, Korea

S. Chang, T.Y. Kim, S.K. Nam

Kyungpook National University, Daegu, Korea

D.H. Kim, G.N. Kim, J.E. Kim, D.J. Kong, S. Lee, Y.D. Oh, H. Park, D.C. Son

Chonnam National University, Institute for Universe and Elementary Particles, Kwangju, Korea

J.Y. Kim, Zero J. Kim, S. Song

Korea University, Seoul, Korea

S. Choi, D. Gyun, B. Hong, M. Jo, H. Kim, Y. Kim, K.S. Lee, S.K. Park, Y. Roh

University of Seoul, Seoul, Korea

M. Choi, J.H. Kim, C. Park, I.C. Park, S. Park, G. Ryu

Sungkyunkwan University, Suwon, Korea

Y. Choi, Y.K. Choi, J. Goh, M.S. Kim, E. Kwon, B. Lee, J. Lee, S. Lee, H. Seo, I. Yu

Vilnius University, Vilnius, Lithuania

A. Juodagalvis

University of Malaya Jabatan Fizik, Kuala Lumpur, Malaysia

J.R. Komaragiri

Centro de Investigacion y de Estudios Avanzados del IPN, Mexico City, Mexico

H. Castilla-Valdez, E. De La Cruz-Burelo, I. Heredia-de La Cruz[31], R. Lopez-Fernandez, J. Martínez-Ortega, A. Sanchez-Hernandez, L.M. Villasenor-Cendejas

Universidad Iberoamericana, Mexico City, Mexico

S. Carrillo Moreno, F. Vazquez Valencia

Benemerita Universidad Autonoma de Puebla, Puebla, Mexico

H.A. Salazar Ibarguen

Universidad Autónoma de San Luis Potosí, San Luis Potosí, Mexico

E. Casimiro Linares, A. Morelos Pineda

University of Auckland, Auckland, New Zealand

D. Krofcheck

University of Canterbury, Christchurch, New Zealand

P.H. Butler, R. Doesburg, S. Reucroft, H. Silverwood

National Centre for Physics, Quaid-I-Azam University, Islamabad, Pakistan

M. Ahmad, M.I. Asghar, J. Butt, H.R. Hoorani, S. Khalid, W.A. Khan, T. Khurshid, S. Qazi, M.A. Shah, M. Shoaib

National Centre for Nuclear Research, Swierk, Poland

H. Bialkowska, M. Bluj[32], B. Boimska, T. Frueboes, M. Górski, M. Kazana, K. Nawrocki, K. Romanowska-Rybinska, M. Szleper, G. Wrochna, P. Zalewski

Institute of Experimental Physics, Faculty of Physics, University of Warsaw, Warsaw, Poland

G. Brona, K. Bunkowski, M. Cwiok, W. Dominik, K. Doroba, A. Kalinowski, M. Konecki, J. Krolikowski, M. Misiura, W. Wolszczak

Laboratório de Instrumentação e Física Experimental de Partículas, Lisboa, Portugal

P. Bargassa, C. Beirão Da Cruz E Silva, P. Faccioli, P.G. Ferreira Parracho, M. Gallinaro, F. Nguyen, J. Rodrigues Antunes, J. Seixas[2], J. Varela, P. Vischia

Joint Institute for Nuclear Research, Dubna, Russia

P. Bunin, M. Gavrilenko, I. Golutvin, I. Gorbunov, A. Kamenev, V. Karjavin, V. Konoplyanikov, G. Kozlov, A. Lanev, A. Malakhov, V. Matveev[33], P. Moisenz, V. Palichik, V. Perelygin, S. Shmatov, N. Skatchkov, V. Smirnov, A. Zarubin

Petersburg Nuclear Physics Institute, Gatchina (St. Petersburg), Russia

V. Golovtsov, Y. Ivanov, V. Kim, P. Levchenko, V. Murzin, V. Oreshkin, I. Smirnov, V. Sulimov, L. Uvarov, S. Vavilov, A. Vorobyev, An. Vorobyev

Institute for Nuclear Research, Moscow, Russia

Yu. Andreev, A. Dermenev, S. Gninenko, N. Golubev, M. Kirsanov, N. Krasnikov, A. Pashenkov, D. Tlisov, A. Toropin

Institute for Theoretical and Experimental Physics, Moscow, Russia

V. Epshteyn, V. Gavrilov, N. Lychkovskaya, V. Popov, G. Safronov, S. Semenov, A. Spiridonov, V. Stolin, E. Vlasov, A. Zhokin

P.N. Lebedev Physical Institute, Moscow, Russia

V. Andreev, M. Azarkin, I. Dremin, M. Kirakosyan, A. Leonidov, G. Mesyats, S.V. Rusakov, A. Vinogradov

Skobeltsyn Institute of Nuclear Physics, Lomonosov Moscow State University, Moscow, Russia

A. Belyaev, E. Boos, M. Dubinin[7], A. Ershov, L. Khein, V. Klyukhin, O. Kodolova, I. Lokhtin, S. Obraztsov, S. Petrushanko, A. Proskuryakov, V. Savrin, A. Snigirev

State Research Center of Russian Federation, Institute for High Energy Physics, Protvino, Russia

I. Azhgirey, I. Bayshev, S. Bitioukov, V. Kachanov, A. Kalinin, D. Konstantinov, V. Krychkine, V. Petrov, R. Ryutin, A. Sobol, L. Tourtchanovitch, S. Troshin, N. Tyurin, A. Uzunian, A. Volkov

University of Belgrade, Faculty of Physics and Vinca Institute of Nuclear Sciences, Belgrade, Serbia

P. Adzic[34], M. Djordjevic, M. Ekmedzic, J. Milosevic

Centro de Investigaciones Energéticas Medioambientales y Tecnológicas (CIEMAT), Madrid, Spain

M. Aguilar-Benitez, J. Alcaraz Maestre, C. Battilana, E. Calvo, M. Cerrada, M. Chamizo Llatas[2], N. Colino, B. De La Cruz, A. Delgado Peris, D. Domínguez Vázquez, C. Fernandez Bedoya, J.P. Fernández Ramos, A. Ferrando, J. Flix, M.C. Fouz, P. Garcia-Abia, O. Gonzalez Lopez, S. Goy Lopez, J.M. Hernandez, M.I. Josa, G. Merino, E. Navarro De Martino, J. Puerta Pelayo, A. Quintario Olmeda, I. Redondo, L. Romero, M.S. Soares, C. Willmott

Universidad Autónoma de Madrid, Madrid, Spain

C. Albajar, J.F. de Trocóniz, M. Missiroli

Universidad de Oviedo, Oviedo, Spain

H. Brun, J. Cuevas, J. Fernandez Menendez, S. Folgueras, I. Gonzalez Caballero, L. Lloret Iglesias

Instituto de Física de Cantabria (IFCA), CSIC-Universidad de Cantabria, Santander, Spain

J.A. Brochero Cifuentes, I.J. Cabrillo, A. Calderon, S.H. Chuang, J. Duarte Campderros, M. Fernandez, G. Gomez, J. Gonzalez Sanchez, A. Graziano, A. Lopez Virto, J. Marco, R. Marco, C. Martinez Rivero, F. Matorras, F.J. Munoz Sanchez, J. Piedra Gomez, T. Rodrigo, A.Y. Rodríguez-Marrero, A. Ruiz-Jimeno, L. Scodellaro, I. Vila, R. Vilar Cortabitarte

CERN, European Organization for Nuclear Research, Geneva, Switzerland

D. Abbaneo, E. Auffray, G. Auzinger, M. Bachtis, P. Baillon, A.H. Ball, D. Barney, J. Bendavid, L. Benhabib, J.F. Benitez, C. Bernet[8], G. Bianchi, P. Bloch, A. Bocci, A. Bonato, O. Bondu, C. Botta, H. Breuker, T. Camporesi, G. Cerminara, T. Christiansen, J.A. Coarasa Perez, S. Colafranceschi[35], M. D'Alfonso, D. d'Enterria, A. Dabrowski, A. David, F. De Guio, A. De Roeck, S. De Visscher, S. Di Guida, M. Dobson, N. Dupont-Sagorin, A. Elliott-Peisert, J. Eugster, G. Franzoni, W. Funk, M. Giffels, D. Gigi, K. Gill, M. Girone, M. Giunta, F. Glege, R. Gomez-Reino Garrido, S. Gowdy, R. Guida, J. Hammer, M. Hansen, P. Harris, V. Innocente, P. Janot, E. Karavakis, K. Kousouris, K. Krajczar, P. Lecoq, C. Lourenço, N. Magini, L. Malgeri, M. Mannelli, L. Masetti, F. Meijers, S. Mersi, E. Meschi, F. Moortgat, M. Mulders, P. Musella, L. Orsini, E. Palencia Cortezon, E. Perez, L. Perrozzi, A. Petrilli, G. Petrucciani, A. Pfeiffer, M. Pierini, M. Pimiä, D. Piparo, M. Plagge, A. Racz, W. Reece, G. Rolandi[36], M. Rovere, H. Sakulin, F. Santanastasio, C. Schäfer, C. Schwick, S. Sekmen, A. Sharma, P. Siegrist, P. Silva, M. Simon, P. Sphicas[37], J. Steggemann, B. Stieger, M. Stoye, A. Tsirou, G.I. Veres[20], J.R. Vlimant, H.K. Wöhri, W.D. Zeuner

Paul Scherrer Institut, Villigen, Switzerland

W. Bertl, K. Deiters, W. Erdmann, R. Horisberger, Q. Ingram, H.C. Kaestli, S. König, D. Kotlinski, U. Langenegger, D. Renker, T. Rohe

Institute for Particle Physics, ETH Zurich, Zurich, Switzerland

F. Bachmair, L. Bäni, L. Bianchini, P. Bortignon, M.A. Buchmann, B. Casal, N. Chanon, A. Deisher, G. Dissertori, M. Dittmar, M. Donegà, M. Dünser, P. Eller, C. Grab, D. Hits, W. Lustermann, B. Mangano, A.C. Marini, P. Martinez Ruiz del Arbol, D. Meister, N. Mohr, C. Nägeli[38], P. Nef, F. Nessi-Tedaldi, F. Pandolfi, L. Pape, F. Pauss, M. Peruzzi, M. Quittnat, F.J. Ronga, M. Rossini, A. Starodumov[39], M. Takahashi, L. Tauscher[†], K. Theofilatos, D. Treille, R. Wallny, H.A. Weber

Universität Zürich, Zurich, Switzerland

C. Amsler[40], V. Chiochia, A. De Cosa, C. Favaro, A. Hinzmann, T. Hreus, M. Ivova Rikova, B. Kilminster, B. Millan Mejias, J. Ngadiuba, P. Robmann, H. Snoek, S. Taroni, M. Verzetti, Y. Yang

National Central University, Chung-Li, Taiwan

M. Cardaci, K.H. Chen, C. Ferro, C.M. Kuo, S.W. Li, W. Lin, Y.J. Lu, R. Volpe, S.S. Yu

National Taiwan University (NTU), Taipei, Taiwan

P. Bartalini, P. Chang, Y.H. Chang, Y.W. Chang, Y. Chao, K.F. Chen, P.H. Chen, C. Dietz, U. Grundler, W.-S. Hou, Y. Hsiung, K.Y. Kao, Y.J. Lei, Y.F. Liu, R.-S. Lu, D. Majumder, E. Petrakou, X. Shi, J.G. Shiu, Y.M. Tzeng, M. Wang, R. Wilken

Chulalongkorn University, Bangkok, Thailand

B. Asavapibhop, N. Suwonjandee

Cukurova University, Adana, Turkey

A. Adiguzel, M.N. Bakirci[41], S. Cerci[42], C. Dozen, I. Dumanoglu, E. Eskut, S. Girgis, G. Gokbulut, E. Gurpinar, I. Hos, E.E. Kangal, A. Kayis Topaksu, G. Onengut[43], K. Ozdemir, S. Ozturk[41], A. Polatoz, K. Sogut[44], D. Sunar Cerci[42], B. Tali[42], H. Topakli[41], M. Vergili

Middle East Technical University, Physics Department, Ankara, Turkey

I.V. Akin, T. Aliev, B. Bilin, S. Bilmis, M. Deniz, H. Gamsizkan, A.M. Guler, G. Karapinar[45], K. Ocalan, A. Ozpineci, M. Serin, R. Sever, U.E. Surat, M. Yalvac, M. Zeyrek

Bogazici University, Istanbul, Turkey

E. Gülmez, B. Isildak[46], M. Kaya[47], O. Kaya[47], S. Ozkorucuklu[48]

Istanbul Technical University, Istanbul, Turkey

H. Bahtiyar[49], E. Barlas, K. Cankocak, Y.O. Günaydin[50], F.I. Vardarlı, M. Yücel

National Scientific Center, Kharkov Institute of Physics and Technology, Kharkov, Ukraine

L. Levchuk, P. Sorokin

University of Bristol, Bristol, United Kingdom

J.J. Brooke, E. Clement, D. Cussans, H. Flacher, R. Frazier, J. Goldstein, M. Grimes, G.P. Heath, H.F. Heath, J. Jacob, L. Kreczko, C. Lucas, Z. Meng, D.M. Newbold[51], S. Paramesvaran, A. Poll, S. Senkin, V.J. Smith, T. Williams

Rutherford Appleton Laboratory, Didcot, United Kingdom

K.W. Bell, A. Belyaev[52], C. Brew, R.M. Brown, D.J.A. Cockerill, J.A. Coughlan, K. Harder, S. Harper, J. Ilic, E. Olaiya, D. Petyt, C.H. Shepherd-Themistocleous, A. Thea, I.R. Tomalin, W.J. Womersley, S.D. Worm

Imperial College, London, United Kingdom

M. Baber, R. Bainbridge, O. Buchmuller, D. Burton, D. Colling, N. Cripps, M. Cutajar, P. Dauncey, G. Davies, M. Della Negra, W. Ferguson, J. Fulcher, D. Futyan, A. Gilbert, A. Guneratne Bryer, G. Hall, Z. Hatherell, J. Hays, G. Iles, M. Jarvis, G. Karapostoli, M. Kenzie, R. Lane, R. Lucas[51], L. Lyons, A.-M. Magnan, J. Marrouche, B. Mathias, R. Nandi, J. Nash, A. Nikitenko[39], J. Pela, M. Pesaresi, K. Petridis, M. Pioppi[53], D.M. Raymond, S. Rogerson, A. Rose, C. Seez, P. Sharp[†], A. Sparrow, A. Tapper, M. Vazquez Acosta, T. Virdee, S. Wakefield, N. Wardle

Brunel University, Uxbridge, United Kingdom

J.E. Cole, P.R. Hobson, A. Khan, P. Kyberd, D. Leggat, D. Leslie, W. Martin, I.D. Reid, P. Symonds, L. Teodorescu, M. Turner

Baylor University, Waco, USA

J. Dittmann, K. Hatakeyama, A. Kasmi, H. Liu, T. Scarborough

The University of Alabama, Tuscaloosa, USA

O. Charaf, S.I. Cooper, C. Henderson, P. Rumerio

Boston University, Boston, USA

A. Avetisyan, T. Bose, C. Fantasia, A. Heister, P. Lawson, D. Lazic, J. Rohlf, D. Sperka, J. St. John, L. Sulak

Brown University, Providence, USA

J. Alimena, S. Bhattacharya, G. Christopher, D. Cutts, Z. Demiragli, A. Ferapontov, A. Garabedian, U. Heintz, S. Jabeen, G. Kukartsev, E. Laird, G. Landsberg, M. Luk, M. Narain, M. Segala, T. Sinthuprasith, T. Speer, J. Swanson

University of California, Davis, Davis, USA

R. Breedon, G. Breto, M. Calderon De La Barca Sanchez, S. Chauhan, M. Chertok, J. Conway, R. Conway, P.T. Cox, R. Erbacher, M. Gardner, W. Ko, A. Kopecky, R. Lander, T. Miceli, D. Pellett, J. Pilot, F. Ricci-Tam, B. Rutherford, M. Searle, S. Shalhout, J. Smith, M. Squires, M. Tripathi, S. Wilbur, R. Yohay

University of California, Los Angeles, USA

V. Andreev, D. Cline, R. Cousins, S. Erhan, P. Everaerts, C. Farrell, M. Felcini, J. Hauser, M. Ignatenko, C. Jarvis, G. Rakness, P. Schlein[†], E. Takasugi, V. Valuev, M. Weber

University of California, Riverside, Riverside, USA

J. Babb, R. Clare, J. Ellison, J.W. Gary, G. Hanson, J. Heilman, P. Jandir, F. Lacroix, H. Liu, O.R. Long, A. Luthra, M. Malberti, H. Nguyen, A. Shrinivas, J. Sturdy, S. Sumowidagdo, S. Wimpenny

University of California, San Diego, La Jolla, USA

W. Andrews, J.G. Branson, G.B. Cerati, S. Cittolin, R.T. D'Agnolo, D. Evans, A. Holzner, R. Kelley, D. Kovalskyi, M. Lebourgeois, J. Letts, I. Macneill, S. Padhi, C. Palmer, M. Pieri, M. Sani, V. Sharma, S. Simon, E. Sudano, M. Tadel, Y. Tu, A. Vartak, S. Wasserbaech[54], F. Würthwein, A. Yagil, J. Yoo

University of California, Santa Barbara, Santa Barbara, USA

D. Barge, C. Campagnari, T. Danielson, K. Flowers, P. Geffert, C. George, F. Golf, J. Incandela, C. Justus, R. Magaña Villalba, N. Mccoll, V. Pavlunin, J. Richman, R. Rossin, D. Stuart, W. To, C. West

California Institute of Technology, Pasadena, USA

A. Apresyan, A. Bornheim, J. Bunn, Y. Chen, E. Di Marco, J. Duarte, D. Kcira, A. Mott, H.B. Newman, C. Pena, C. Rogan, M. Spiropulu, V. Timciuc, R. Wilkinson, S. Xie, R.Y. Zhu

Carnegie Mellon University, Pittsburgh, USA

V. Azzolini, A. Calamba, R. Carroll, T. Ferguson, Y. Iiyama, D.W. Jang, M. Paulini, J. Russ, H. Vogel, I. Vorobiev

University of Colorado at Boulder, Boulder, USA

J.P. Cumalat, B.R. Drell, W.T. Ford, A. Gaz, E. Luiggi Lopez, U. Nauenberg, J.G. Smith, K. Stenson, K.A. Ulmer, S.R. Wagner

Cornell University, Ithaca, USA

J. Alexander, A. Chatterjee, N. Eggert, L.K. Gibbons, W. Hopkins, A. Khukhunaishvili, B. Kreis, N. Mirman, G. Nicolas Kaufman, J.R. Patterson, A. Ryd, E. Salvati, W. Sun, W.D. Teo, J. Thom, J. Thompson, J. Tucker, Y. Weng, L. Winstrom, P. Wittich

Fairfield University, Fairfield, USA

D. Winn

Fermi National Accelerator Laboratory, Batavia, USA

S. Abdullin, M. Albrow, J. Anderson, G. Apollinari, L.A.T. Bauerdick, A. Beretvas, J. Berryhill, P.C. Bhat, K. Burkett, J.N. Butler, V. Chetluru, H.W.K. Cheung, F. Chlebana, S. Cihangir, V.D. Elvira, I. Fisk, J. Freeman, Y. Gao, E. Gottschalk, L. Gray, D. Green, S. Grünendahl, O. Gutsche, D. Hare, R.M. Harris, J. Hirschauer, B. Hooberman, S. Jindariani, M. Johnson, U. Joshi, K. Kaadze, B. Klima, S. Kwan, J. Linacre, D. Lincoln, R. Lipton, J. Lykken, K. Maeshima, J.M. Marraffino, V.I. Martinez Outschoorn, S. Maruyama, D. Mason, P. McBride, K. Mishra, S. Mrenna, Y. Musienko[33], S. Nahn, C. Newman-Holmes, V. O'Dell, O. Prokofyev, N. Ratnikova, E. Sexton-Kennedy, S. Sharma, W.J. Spalding, L. Spiegel, L. Taylor, S. Tkaczyk, N.V. Tran, L. Uplegger, E.W. Vaandering, R. Vidal, A. Whitbeck, J. Whitmore, W. Wu, F. Yang, J.C. Yun

University of Florida, Gainesville, USA

D. Acosta, P. Avery, D. Bourilkov, T. Cheng, S. Das, M. De Gruttola, G.P. Di Giovanni, D. Dobur, R.D. Field, M. Fisher, Y. Fu, I.K. Furic, J. Hugon, B. Kim, J. Konigsberg,

A. Korytov, A. Kropivnitskaya, T. Kypreos, J.F. Low, K. Matchev, P. Milenovic[55], G. Mitselmakher, L. Muniz, A. Rinkevicius, L. Shchutska, N. Skhirtladze, M. Snowball, J. Yelton, M. Zakaria

Florida International University, Miami, USA

V. Gaultney, S. Hewamanage, S. Linn, P. Markowitz, G. Martinez, J.L. Rodriguez

Florida State University, Tallahassee, USA

T. Adams, A. Askew, J. Bochenek, J. Chen, B. Diamond, J. Haas, S. Hagopian, V. Hagopian, K.F. Johnson, H. Prosper, V. Veeraraghavan, M. Weinberg

Florida Institute of Technology, Melbourne, USA

M.M. Baarmand, B. Dorney, M. Hohlmann, H. Kalakhety, F. Yumiceva

University of Illinois at Chicago (UIC), Chicago, USA

M.R. Adams, L. Apanasevich, V.E. Bazterra, R.R. Betts, I. Bucinskaite, R. Cavanaugh, O. Evdokimov, L. Gauthier, C.E. Gerber, D.J. Hofman, S. Khalatyan, P. Kurt, D.H. Moon, C. O'Brien, C. Silkworth, P. Turner, N. Varelas

The University of Iowa, Iowa City, USA

U. Akgun, E.A. Albayrak[49], B. Bilki[56], W. Clarida, K. Dilsiz, F. Duru, M. Haytmyradov, J.-P. Merlo, H. Mermerkaya[57], A. Mestvirishvili, A. Moeller, J. Nachtman, H. Ogul, Y. Onel, F. Ozok[49], S. Sen, P. Tan, E. Tiras, J. Wetzel, T. Yetkin[58], K. Yi

Johns Hopkins University, Baltimore, USA

B.A. Barnett, B. Blumenfeld, S. Bolognesi, D. Fehling, A.V. Gritsan, P. Maksimovic, C. Martin, M. Swartz

The University of Kansas, Lawrence, USA

P. Baringer, A. Bean, G. Benelli, R.P. Kenny III, M. Murray, D. Noonan, S. Sanders, J. Sekaric, R. Stringer, Q. Wang, J.S. Wood

Kansas State University, Manhattan, USA

A.F. Barfuss, I. Chakaberia, A. Ivanov, S. Khalil, M. Makouski, Y. Maravin, L.K. Saini, S. Shrestha, I. Svintradze

Lawrence Livermore National Laboratory, Livermore, USA

J. Gronberg, D. Lange, F. Rebassoo, D. Wright

University of Maryland, College Park, USA

A. Baden, B. Calvert, S.C. Eno, J.A. Gomez, N.J. Hadley, R.G. Kellogg, T. Kolberg, Y. Lu, M. Marionneau, A.C. Mignerey, K. Pedro, A. Skuja, J. Temple, M.B. Tonjes, S.C. Tonwar

Massachusetts Institute of Technology, Cambridge, USA

A. Apyan, R. Barbieri, G. Bauer, W. Busza, I.A. Cali, M. Chan, L. Di Matteo, V. Dutta, G. Gomez Ceballos, M. Goncharov, D. Gulhan, M. Klute, Y.S. Lai, Y.-J. Lee, A. Levin, P.D. Luckey, T. Ma, C. Paus, D. Ralph, C. Roland, G. Roland, G.S.F. Stephans, F. Stöckli, K. Sumorok, D. Velicanu, J. Veverka, B. Wyslouch, M. Yang, A.S. Yoon, M. Zanetti, V. Zhukova

University of Minnesota, Minneapolis, USA

B. Dahmes, A. De Benedetti, A. Gude, S.C. Kao, K. Klapoetke, Y. Kubota, J. Mans, N. Pastika, R. Rusack, A. Singovsky, N. Tambe, J. Turkewitz

University of Mississippi, Oxford, USA

J.G. Acosta, L.M. Cremaldi, R. Kroeger, S. Oliveros, L. Perera, R. Rahmat, D.A. Sanders, D. Summers

University of Nebraska-Lincoln, Lincoln, USA

E. Avdeeva, K. Bloom, S. Bose, D.R. Claes, A. Dominguez, R. Gonzalez Suarez, J. Keller, D. Knowlton, I. Kravchenko, J. Lazo-Flores, S. Malik, F. Meier, G.R. Snow

State University of New York at Buffalo, Buffalo, USA

J. Dolen, A. Godshalk, I. Iashvili, S. Jain, A. Kharchilava, A. Kumar, S. Rappoccio, Z. Wan

Northeastern University, Boston, USA

G. Alverson, E. Barberis, D. Baumgartel, M. Chasco, J. Haley, A. Massironi, D. Nash, T. Orimoto, D. Trocino, D. Wood, J. Zhang

Northwestern University, Evanston, USA

A. Anastassov, K.A. Hahn, A. Kubik, L. Lusito, N. Mucia, N. Odell, B. Pollack, A. Pozdnyakov, M. Schmitt, S. Stoynev, K. Sung, M. Velasco, S. Won

University of Notre Dame, Notre Dame, USA

D. Berry, A. Brinkerhoff, K.M. Chan, A. Drozdetskiy, M. Hildreth, C. Jessop, D.J. Karmgard, N. Kellams, J. Kolb, K. Lannon, W. Luo, S. Lynch, N. Marinelli, D.M. Morse, T. Pearson, M. Planer, R. Ruchti, J. Slaunwhite, N. Valls, M. Wayne, M. Wolf, A. Woodard

The Ohio State University, Columbus, USA

L. Antonelli, B. Bylsma, L.S. Durkin, S. Flowers, C. Hill, R. Hughes, K. Kotov, T.Y. Ling, D. Puigh, M. Rodenburg, G. Smith, C. Vuosalo, B.L. Winer, H. Wolfe, H.W. Wulsin

Princeton University, Princeton, USA

E. Berry, P. Elmer, V. Halyo, P. Hebda, J. Hegeman, A. Hunt, P. Jindal, S.A. Koay, P. Lujan, D. Marlow, T. Medvedeva, M. Mooney, J. Olsen, P. Piroué, X. Quan, A. Raval, H. Saka, D. Stickland, C. Tully, J.S. Werner, S.C. Zenz, A. Zuranski

University of Puerto Rico, Mayaguez, USA

E. Brownson, A. Lopez, H. Mendez, J.E. Ramirez Vargas

Purdue University, West Lafayette, USA

E. Alagoz, D. Benedetti, G. Bolla, D. Bortoletto, M. De Mattia, A. Everett, Z. Hu, M. Jones, K. Jung, M. Kress, N. Leonardo, D. Lopes Pegna, V. Maroussov, P. Merkel, D.H. Miller, N. Neumeister, B.C. Radburn-Smith, I. Shipsey, D. Silvers, A. Svyatkovskiy, F. Wang, W. Xie, L. Xu, H.D. Yoo, J. Zablocki, Y. Zheng

Purdue University Calumet, Hammond, USA

N. Parashar

Rice University, Houston, USA

A. Adair, B. Akgun, K.M. Ecklund, F.J.M. Geurts, W. Li, B. Michlin, B.P. Padley, R. Redjimi, J. Roberts, J. Zabel

University of Rochester, Rochester, USA

B. Betchart, A. Bodek, R. Covarelli, P. de Barbaro, R. Demina, Y. Eshaq, T. Ferbel, A. Garcia-Bellido, P. Goldenzweig, J. Han, A. Harel, D.C. Miner, G. Petrillo, D. Vishnevskiy, M. Zielinski

The Rockefeller University, New York, USA

A. Bhatti, R. Ciesielski, L. Demortier, K. Goulianos, G. Lungu, S. Malik, C. Mesropian

Rutgers, The State University of New Jersey, Piscataway, USA

S. Arora, A. Barker, J.P. Chou, C. Contreras-Campana, E. Contreras-Campana, D. Duggan, D. Ferencek, Y. Gershtein, R. Gray, E. Halkiadakis, D. Hidas, A. Lath, S. Panwalkar, M. Park, R. Patel, V. Rekovic, J. Robles, S. Salur, S. Schnetzer, C. Seitz, S. Somalwar, R. Stone, S. Thomas, P. Thomassen, M. Walker

University of Tennessee, Knoxville, USA

K. Rose, S. Spanier, Z.C. Yang, A. York

Texas A&M University, College Station, USA

O. Bouhali[59], R. Eusebi, W. Flanagan, J. Gilmore, T. Kamon[60], V. Khotilovich, V. Krutelyov, R. Montalvo, I. Osipenkov, Y. Pakhotin, A. Perloff, J. Roe, A. Safonov, T. Sakuma, I. Suarez, A. Tatarinov, D. Toback

Texas Tech University, Lubbock, USA

N. Akchurin, C. Cowden, J. Damgov, C. Dragoiu, P.R. Dudero, K. Kovitanggoon, S. Kunori, S.W. Lee, T. Libeiro, I. Volobouev

Vanderbilt University, Nashville, USA

E. Appelt, A.G. Delannoy, S. Greene, A. Gurrola, W. Johns, C. Maguire, Y. Mao, A. Melo, M. Sharma, P. Sheldon, B. Snook, S. Tuo, J. Velkovska

University of Virginia, Charlottesville, USA

M.W. Arenton, S. Boutle, B. Cox, B. Francis, J. Goodell, R. Hirosky, A. Ledovskoy, C. Lin, C. Neu, J. Wood

Wayne State University, Detroit, USA

S. Gollapinni, R. Harr, P.E. Karchin, C. Kottachchi Kankanamge Don, P. Lamichhane

University of Wisconsin, Madison, USA

D.A. Belknap, L. Borrello, D. Carlsmith, M. Cepeda, S. Dasu, S. Duric, E. Friis, M. Grothe, R. Hall-Wilton, M. Herndon, A. Hervé, P. Klabbers, J. Klukas, A. Lanaro, A. Levine, R. Loveless, A. Mohapatra, I. Ojalvo, T. Perry, G.A. Pierro, G. Polese, I. Ross, A. Sakharov, T. Sarangi, A. Savin, W.H. Smith

†: Deceased

1: Also at Vienna University of Technology, Vienna, Austria

2: Also at CERN, European Organization for Nuclear Research, Geneva, Switzerland

3: Also at Institut Pluridisciplinaire Hubert Curien, Université de Strasbourg, Université de Haute Alsace Mulhouse, CNRS/IN2P3, Strasbourg, France

4: Also at National Institute of Chemical Physics and Biophysics, Tallinn, Estonia

5: Also at Skobeltsyn Institute of Nuclear Physics, Lomonosov Moscow State University, Moscow, Russia

6: Also at Universidade Estadual de Campinas, Campinas, Brazil

7: Also at California Institute of Technology, Pasadena, USA

8: Also at Laboratoire Leprince-Ringuet, Ecole Polytechnique, IN2P3-CNRS, Palaiseau, France

9: Also at Zewail City of Science and Technology, Zewail, Egypt

10: Also at Suez Canal University, Suez, Egypt

11: Also at Cairo University, Cairo, Egypt

12: Also at Fayoum University, El-Fayoum, Egypt

13: Also at British University in Egypt, Cairo, Egypt

14: Now at Ain Shams University, Cairo, Egypt

15: Also at Université de Haute Alsace, Mulhouse, France

16: Also at Joint Institute for Nuclear Research, Dubna, Russia

17: Also at Brandenburg University of Technology, Cottbus, Germany

18: Also at The University of Kansas, Lawrence, USA

19: Also at Institute of Nuclear Research ATOMKI, Debrecen, Hungary

20: Also at Eötvös Loránd University, Budapest, Hungary

21: Also at Tata Institute of Fundamental Research - HECR, Mumbai, India

22: Now at King Abdulaziz University, Jeddah, Saudi Arabia

23: Also at University of Visva-Bharati, Santiniketan, India

24: Also at University of Ruhuna, Matara, Sri Lanka

25: Also at Isfahan University of Technology, Isfahan, Iran

26: Also at Sharif University of Technology, Tehran, Iran

27: Also at Plasma Physics Research Center, Science and Research Branch, Islamic Azad University, Tehran, Iran

28: Also at Università degli Studi di Siena, Siena, Italy

29: Also at Centre National de la Recherche Scientifique (CNRS) - IN2P3, Paris, France

30: Also at Purdue University, West Lafayette, USA

31: Also at Universidad Michoacana de San Nicolas de Hidalgo, Morelia, Mexico

32: Also at National Centre for Nuclear Research, Swierk, Poland

33: Also at Institute for Nuclear Research, Moscow, Russia

34: Also at Faculty of Physics, University of Belgrade, Belgrade, Serbia

35: Also at Facoltà Ingegneria, Università di Roma, Roma, Italy

36: Also at Scuola Normale e Sezione dell'INFN, Pisa, Italy

37: Also at University of Athens, Athens, Greece

38: Also at Paul Scherrer Institut, Villigen, Switzerland

39: Also at Institute for Theoretical and Experimental Physics, Moscow, Russia

40: Also at Albert Einstein Center for Fundamental Physics, Bern, Switzerland

41: Also at Gaziosmanpasa University, Tokat, Turkey

42: Also at Adiyaman University, Adiyaman, Turkey

43: Also at Cag University, Mersin, Turkey

44: Also at Mersin University, Mersin, Turkey

45: Also at Izmir Institute of Technology, Izmir, Turkey

46: Also at Ozyegin University, Istanbul, Turkey

47: Also at Kafkas University, Kars, Turkey

48: Also at Istanbul University, Faculty of Science, Istanbul, Turkey

49: Also at Mimar Sinan University, Istanbul, Istanbul, Turkey

50: Also at Kahramanmaras Sütcü Imam University, Kahramanmaras, Turkey

51: Also at Rutherford Appleton Laboratory, Didcot, United Kingdom

52: Also at School of Physics and Astronomy, University of Southampton, Southampton, United Kingdom

53: Also at INFN Sezione di Perugia; Università di Perugia, Perugia, Italy

54: Also at Utah Valley University, Orem, USA

55: Also at University of Belgrade, Faculty of Physics and Vinca Institute of Nuclear Sciences, Belgrade, Serbia

56: Also at Argonne National Laboratory, Argonne, USA

57: Also at Erzincan University, Erzincan, Turkey

58: Also at Yildiz Technical University, Istanbul, Turkey

59: Also at Texas A&M University at Qatar, Doha, Qatar

60: Also at Kyungpook National University, Daegu, Korea